RESOURCE

nature cell biology

Genome-wide association between YAP/TAZ/TEAD and AP-1 at enhancers drives oncogenic growth

Francesca Zanconato[1], Mattia Forcato[2], Giusy Battilana[1], Luca Azzolin[1], Erika Quaranta[1], Beatrice Bodega[3], Antonio Rosato[4,5], Silvio Bicciato[2], Michelangelo Cordenonsi[1,6] and Stefano Piccolo[1,6]

YAP/TAZ are nuclear effectors of the Hippo pathway regulating organ growth and tumorigenesis. Yet, their function as transcriptional regulators remains underinvestigated. By ChIP-seq analyses in breast cancer cells, we discovered that the YAP/TAZ transcriptional response is pervasively mediated by a dual element: TEAD factors, through which YAP/TAZ bind to DNA, co-occupying chromatin with activator protein-1 (AP-1, dimer of JUN and FOS proteins) at composite *cis*-regulatory elements harbouring both TEAD and AP-1 motifs. YAP/TAZ/TEAD and AP-1 form a complex that synergistically activates target genes directly involved in the control of S-phase entry and mitosis. This control occurs almost exclusively from distal enhancers that contact target promoters through chromatin looping. YAP/TAZ-induced oncogenic growth is strongly enhanced by gain of AP-1 and severely blunted by its loss. Conversely, AP-1-promoted skin tumorigenesis is prevented in YAP/TAZ conditional knockout mice. This work highlights a new layer of signalling integration, feeding on YAP/TAZ function at the chromatin level.

YAP/TAZ (refs 1,2) are potent inducers of cell proliferation and are important drivers of tumorigenesis in a number of contexts[3–6]. Yet, the mechanisms underpinning this activity remain enigmatic. Only a handful of direct targets have been described in mammalian cells, leaving largely undefined what are the immediate downstream effectors by which YAP/TAZ exert their biological effects[3]. Moreover, lack of systematic studies results in just a scattered understanding of the transcriptional partners by which nuclear YAP/TAZ control transcription on a genome-wide scale. Also unknown is whether and how, after binding to DNA, YAP/TAZ achieve combinatorial control of gene expression, for example through cooperation with other nuclear oncogenes during YAP/TAZ-driven oncogenic growth.

RESULTS

A genomic map of YAP/TAZ recruitment to chromatin

To elucidate how YAP/TAZ regulate gene expression in tumour cells we performed chromatin immunoprecipitation assays with YAP and TAZ antibodies followed by next-generation sequencing (ChIP-seq) in MDA-MB-231 breast cancer cells, bearing genetic inactivation of the Hippo pathway (*NF2* null)[7]. A total of 7,107 peaks were identified by both antibodies (Fig. 1a). YAP/TAZ-bound regions included the promoters of previously established YAP/TAZ direct targets (*CTGF*, *CYR61*, *ANKRD1*, *AXL*, *AMOTL2*, *AJUBA* and *WTIP*, Supplementary Fig. 1b–d).

YAP/TAZ do not carry a DNA-binding domain, and thus can contact the DNA only indirectly, through transcription factor partners. So far, a number of these partners have been described, including TEAD1-4, RUNX, p73, KLF4, TBX5 and others[3,8–11]. Motif analyses at YAP/TAZ peaks revealed that the main platforms by which YAP/TAZ interact with DNA are TEAD proteins: their consensus sequence was present in at least 75% of YAP/TAZ peaks, typically at the summit of YAP/TAZ peaks (Supplementary Fig. 1e,f). TEAD factors have been repeatedly associated as mediators of YAP/TAZ transcriptional responses[3,9]; surprisingly no motifs for the other proposed DNA-binding platforms of YAP/TAZ were significantly enriched (with the exception of RUNX, found in a minority of peaks; see Supplementary Table 1).

Following these results, we performed a ChIP-seq experiment for endogenous TEAD4 and found that 78% (5,522) of YAP/TAZ peaks overlapped with TEAD4 peaks (Fig. 1b and Supplementary Table 2); furthermore, the summits of TEAD4 peaks coincide with the summit of the corresponding YAP/TAZ peaks (Fig. 1c), indicating that TEAD factors are indeed the main driver for YAP/TAZ recruitment to chromatin. In support of this notion, the signal of TEAD4 peaks

[1]Department of Molecular Medicine, University of Padua School of Medicine, viale Colombo 3, 35126 Padua, Italy. [2]Center for Genome Research, Department of Life Sciences, University of Modena and Reggio Emilia, via G. Campi 287, 41100 Modena, Italy. [3]Genome Biology Unit, Istituto Nazionale di Genetica Molecolare (INGM) 'Romeo and Enrica Invernizzi', via Francesco Sforza 35, Milan 20126, Italy. [4]Department of Surgery, Oncology and Gastroenterology, University of Padua School of Medicine, Via Gattamelata 64, 35126 Padua, Italy. [5]Istituto Oncologico Veneto IOV-IRCCS, Via Gattamelata 64, 35126 Padua, Italy.
[6]Correspondence should be addressed to M.C. or S.P. (e-mail: michelangelo.cordenonsi@unipd.it or piccolo@bio.unipd.it)

Received 20 March 2015; accepted 2 July 2015; published online 10 August 2015; DOI: 10.1038/ncb3216

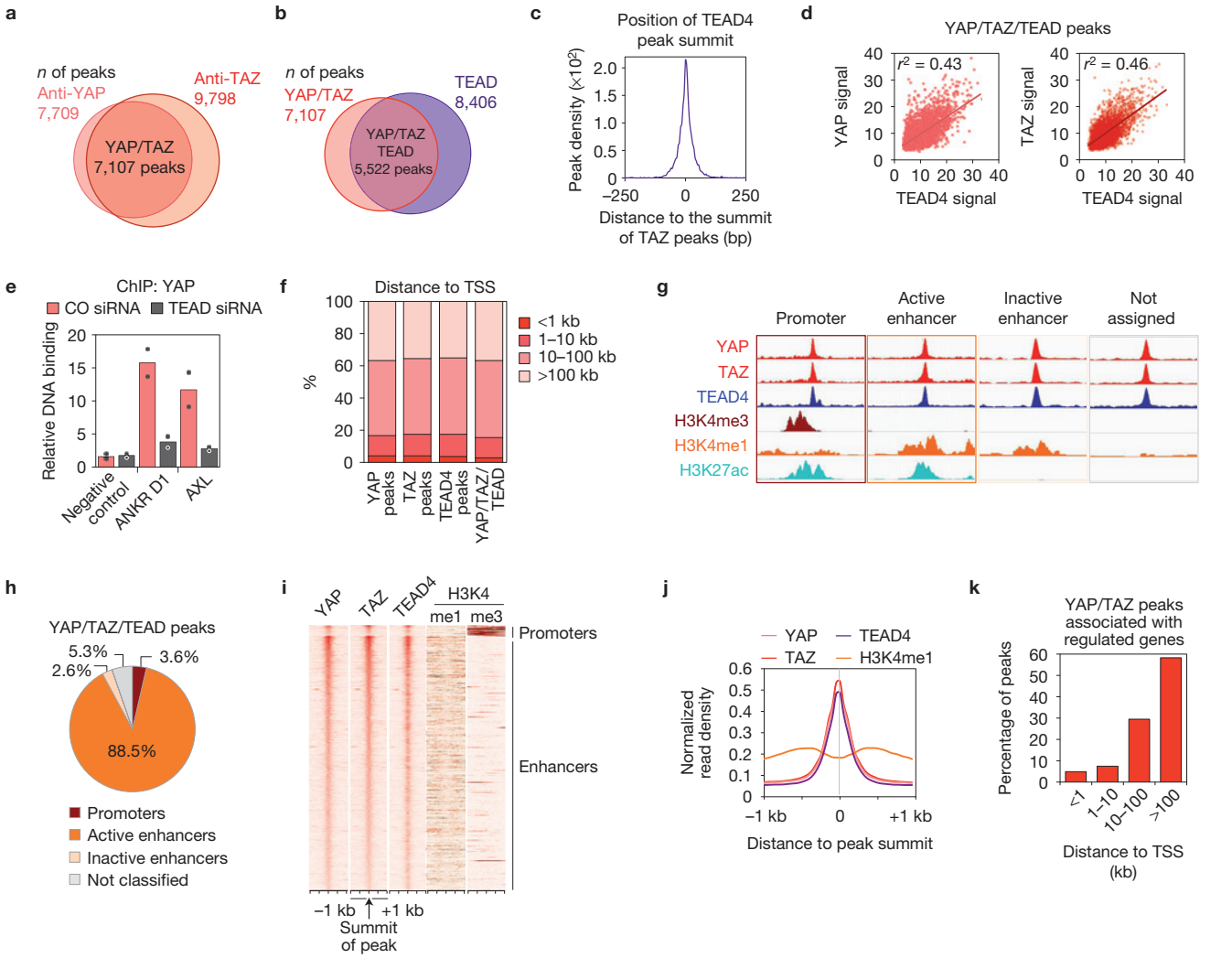

Figure 1 Genome-wide co-localization of YAP, TAZ and TEAD on enhancers. (**a**) Overlap of peaks identified with YAP and TAZ antibodies. See Supplementary Fig. 1a for specificity controls of the antibodies, and Supplementary Table 1 for the results of *de novo* motif finding in YAP/TAZ peaks. (**b**) Overlap of YAP/TAZ peaks and TEAD4 peaks. See Supplementary Fig. 1g for specificity controls of TEAD4 antibody, and Supplementary Fig. 1h for ChIP-seq profiles at positive control loci. (**c**) Position of TEAD4 peak summits relative to the summits of the overlapping YAP/TAZ peaks, in a 500 bp window surrounding the summit of YAP/TAZ peaks. (**d**) Linear correlation between the signal of YAP or TAZ and TEAD4 peaks in the 5,522 shared binding sites. r^2 is the coefficients of determination of the two correlations. (**e**) ChIP-qPCR showing YAP binding to the indicated sites in MDA-MB-231 cells transfected with control (CO siRNA) or TEAD siRNAs (TEAD siRNA A). Relative DNA binding was calculated as fraction of input and normalized to IgG (IgG bars are omitted); data from 2 biological replicates (individual data points and their mean) from one representative experiment are shown. (**f**) Absolute distance of YAP peaks (n=7,709), TAZ peaks (n=9,798), TEAD4 peaks (n=8,406) or overlapping YAP/TAZ/TEAD peaks (n=5,522) to the nearest TSS. (**g**,**h**) Association of YAP/TAZ/TEAD peaks to promoters and enhancers according to ChIP-seq data for histone modifications. (**g**) Scheme illustrating peak classification. (**h**) Fraction of YAP/TAZ/TEAD peaks associated with each category. See Supplementary Fig. 1j for validation of the enhancer/promoter status of a set of YAP/TAZ/TEAD-bound regions. (**i**) Heatmap representing YAP/TAZ/TEAD-binding sites located on promoters (top) and enhancers (bottom). YAP, TAZ and TEAD4 peaks are ranked from the strongest to weakest signal in TAZ ChIP, in a window of ±1 kb centred on the summit of TAZ peaks. H3K4me1 and H3K4me3 signal in the corresponding genomic regions is shown on the right. (**j**) Bimodal distribution of H3K4me1 signal around the summit of YAP/TAZ and TEAD4 peaks. (**k**) Distance between YAP/TAZ/TEAD-binding sites and the TSS of the direct target genes they are associated to. Overall, 635 peaks were associated to 379 genes positively regulated by YAP/TAZ. See Methods for reproducibility of experiments.

is positively correlated with that one of YAP/TAZ peaks (Fig. 1d), and binding of YAP to chromatin is strongly affected by combined knockdown of TEAD1/2/3/4 as assessed by ChIP-qPCR (Fig. 1e).

Global association of YAP/TAZ/TEAD to enhancer elements

We analysed the distribution of YAP-, TAZ- or TEAD-binding sites relative to genes annotated in the human genome, and found that only a minute fraction of peaks mapped close (±1 kilobase (kb)) to transcription start sites (TSSs) whereas most peaks were located farther than 10 kb from the closest TSS (Fig. 1f). Analyses of publicly available TEAD ChIP-seq data revealed that this pattern is conserved in several cancer cell types (Supplementary Fig. 1i).

Owing to their remote location, we questioned whether most YAP/TAZ/TEAD common peaks are located in enhancers. Enhancers

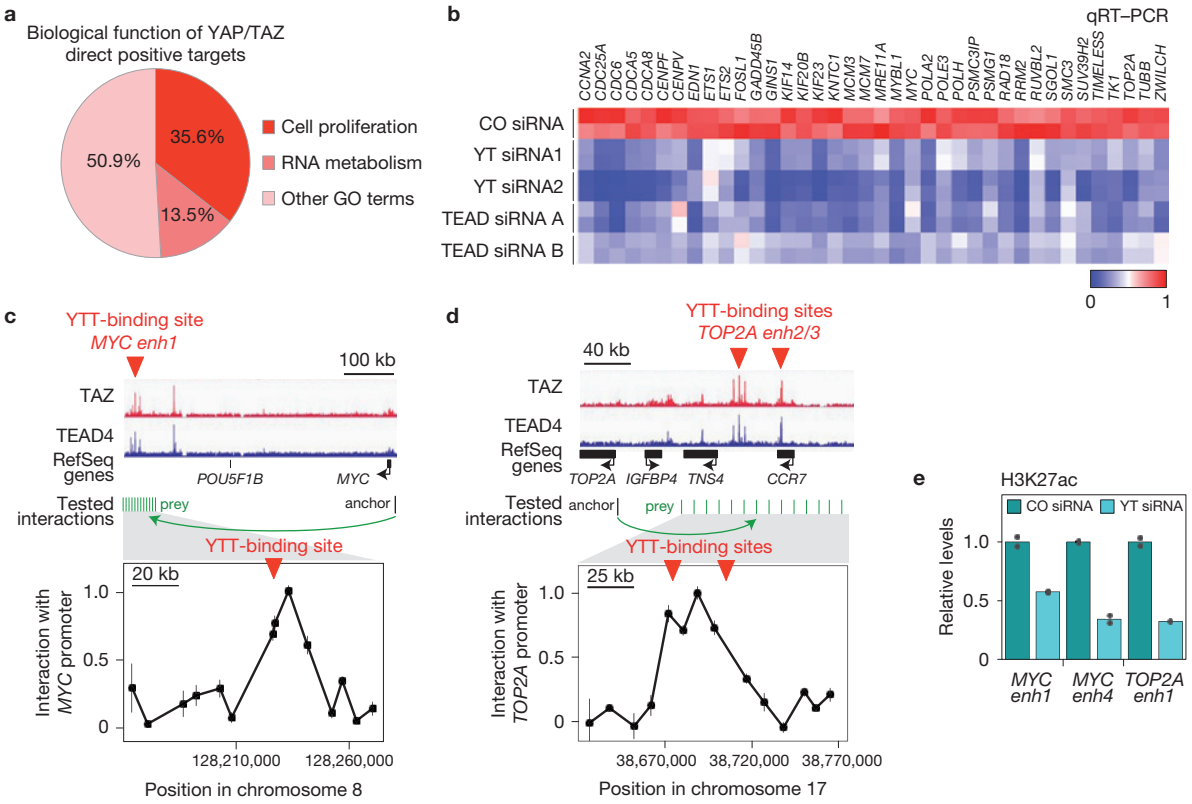

Figure 2 YAP/TAZ/TEAD transcriptional program. (**a**) Biological functions associated to YAP/TAZ direct positive targets, identified by GO terms. (**b**) YAP/TAZ or TEAD depletion impairs the expression of YAP/TAZ/TEAD direct target genes involved in cell proliferation, as evaluated by qRT–PCR (CO siRNA, control siRNA; YT siRNA, YAP/TAZ siRNA). For a subset of genes, the downregulation of the corresponding proteins was also verified by western blot (Supplementary Fig. 2b). See Supplementary Fig. 2a for validation of TEAD siRNAs. (**c**,**d**) Validation of the long-range interaction between YAP/TAZ-occupied enhancers and the promoters of MYC (**c**) and TOP2A (**d**) by DNA looping, using 3C assays in MDA-MB-231 cells. TAZ and TEAD4 ChIP-seq profiles show the position of YAP/TAZ/TEAD-binding sites upstream of MYC or TOP2A genes (here named 'MYC enhancer 1', 'TOP2A enhancer2' 'TOP2A enhancer3'), whereas no YAP/TAZ/TEAD-binding sites were detected close to their TSS. The chart shows the frequency of interaction (measured as crosslinking frequency) between MYC or TOP2A promoter ('anchor') and the indicated sites surrounding YAP/TAZ/TEAD (YTT) peaks (green lines). Interaction frequency is higher close to YAP/TAZ peak. Data points are mean + s.e.m. from $n=3$ biological replicates. See also Supplementary Fig. 2d,e for the additional interactions between MYC and TOP2A promoters and a different set of YAP/TAZ/TEAD-bound enhancers. (**e**) ChIP-qPCR comparing the levels of H3K27ac (normalized to total H3 levels) in MDA-MB-231 cells transfected with control (CO siRNA) or combined YAP/TAZ siRNAs (YT siRNA, a mix of YT siRNA 1 + YT siRNA 2). Data from 2 biological replicates (individual data points and their mean) from one representative experiment are shown. See Methods for reproducibility of experiments.

can be distinguished from promoters by their epigenetic features, that is, relative enrichment of histone H3 monomethylation (H3K4me1) on Lys 4 at enhancers, and trimethylation (H3K4me3) at promoters[12]. ChIP-seq data for these epigenetic marks in MDA-MB-231 cells were recently reported[13], allowing us to compare this map of promoters and enhancers with the location of YAP/TAZ/TEAD4 peaks (Fig. 1g). Notably, only a very small fraction (3.6%) of YAP/TAZ/TEAD4 peaks are located on promoters; instead, 91% of peaks are located in enhancer regions (Fig. 1h,i). Furthermore, most of these enhancers are in an active state as revealed by H3K27 acetylation and reduced nucleosome occupancy at the peak centre, also resulting in a bimodal distribution of H3K4me1 around the peak summit (Fig. 1h–j and Supplementary Fig. 1k).

A YAP/TAZ-regulated transcriptional program driving cell proliferation

We then sought to link YAP/TAZ/TEAD4 peaks to corresponding target genes (Supplementary Fig. 1l). All of the peaks located in promoter regions (201) were assigned to the nearest genes. However, application of this proximity criterion to the distant enhancers bound by YAP/TAZ was questionable, as enhancers can regulate target genes over long distances, often skipping intervening genes. Instead, the specificity of enhancer–promoter associations is dictated by the three-dimensional higher-order chromatin structure, whereby enhancers interact with their target promoters through chromatin looping[12]. Importantly, a recently reported high-resolution map of chromatin interactions (Hi-C) has been shown to predict *bona fide* enhancer–promoter pairs with great accuracy[14]. Notably, most of these long-range chromatin interactions are conserved across cell types[15]. By using the map of enhancer–promoter pairs discovered in ref. 14, we could associate more than half of YAP/YAZ/TEAD4-bound enhancers to a set of 2,957 candidate target genes; considering also the genes with peaks in their promoters, the list extends to 3,089 genes. Of these candidates, 379 are in fact expressed in MDA-MB-231 cells, and in a YAP/TAZ-dependent manner, as determined by Affymetrix profiling of control and YAP/TAZ-depleted cells (using two independent

combinations of siRNAs; Supplementary Table 3). Crucially, most (88.6%) of these *bona fide* YAP/TAZ direct targets are controlled only from distal enhancers, mostly located farther than 100,000 base pairs (bp) from the TSS (Fig. 1k); we further note that these genes could not have been identified by assigning the peak to the closest gene.

To identify the main biological processes regulated by YAP/TAZ, we performed Gene Ontology (GO) analyses on the list of YAP/TAZ direct targets. A large fraction of positive targets (135) are linked to processes related to cell cycle progression (Fig. 2a and Supplementary Tables 4 and 5); YAP/TAZ/TEAD-binding sites are located exclusively on distal enhancers for 115 of these genes, and both on promoters and enhancers for other 11 genes. Other positive targets (13.5% of the total) are connected to RNA metabolism and RNA transport.

The YAP/TAZ/TEAD cell-proliferation program comprises essential factors involved in replication licensing, DNA synthesis and repair (for example, *CDC6*, *GINS1*, *MCM3*, *MCM7*, *POLA2*, *POLE3*, *TOP2A* and *RAD18*), transcriptional regulators of the cell cycle (for example, *ETS1*, *MYC* and *MYBL1*), cyclins and their activators (*CCNA2* and *CDC25A*), and factors required for completion of mitosis (for example, *CENPF*, *CDCA5* and *KIF23*). We selected about 40 of these genes (containing representative genes belonging to each of the above-mentioned categories) and confirmed by quantitative PCR with reverse transcription (qRT–PCR) that their expression depends on YAP/TAZ as well as on TEAD1-4 (Fig. 2b). All of these new YAP/TAZ/TEAD-regulated genes were associated to YAP/TAZ/TEAD peaks located on enhancers (as exemplified in Supplementary Fig. 2c). By chromatin conformation capture (3C) analysis we confirmed that the interaction of YAP/TAZ/TEAD-bound enhancers with *MYC* or *TOP2A* promoters occurs through chromatin looping in MDA-MB-231 cells (Fig. 2c,d and Supplementary Fig. 2d,e), validating the procedure here used to associate distant enhancers to target genes by using Hi-C data. Remarkably, YAP/TAZ are required for the activity of these enhancers, as acetylation of H3K27 in these regions drops in YAP/TAZ-depleted cells (Fig. 2e).

We next aimed to determine the biological validity of these findings. We found that YAP/TAZ-depleted cells stop proliferating and accumulate in the G_1 phase (Fig. 3a,b). These effects are phenocopied by TEAD depletion (Supplementary Fig. 3b,c); moreover, the growth of YAP/TAZ-depleted cells can be fully rescued by reintroduction of wild-type YAP or TAZ, but not by their TEAD-binding-deficient mutants (Fig. 3c and Supplementary Fig. 3d). Together, these results underline the relevance of TEAD as the master determinant of YAP/TAZ-driven proliferation[9].

To investigate the newly identified YAP/TAZ direct targets, we focused on MYC, given its established prominence as a regulator of cell proliferation. As shown in Supplementary Fig. 3e–g, MYC knockdown caused a minor, but significant reduction of cell proliferation and a substantial increase of cells in the G_1 phase, in part phenocopying the requirement of YAP/TAZ. Overexpression of MYC in YAP/TAZ-depleted cells triggered a significant, but only a partial rescue of cell proliferation (Fig. 3d). This indicates that MYC represents an important functional effector of YAP/TAZ in this context; however, MYC alone cannot fully recapitulate the biological effectiveness of YAP/TAZ.

We next sought to determine whether genes identified as YAP/TAZ/TEAD targets in MDA-MB-231 cells are exploited in human breast cancers. YAP/TAZ are required and sufficient to confer malignant traits to more benign tumour cells[16–18]. In line, elevated levels of YAP/TAZ in human breast cancer specimens identify aggressive tumours (defined as high histopathological grade, or 'G3'), and those with worse prognosis[16]. Direct targets of YAP/TAZ/TEAD should thus similarly earmark aggressive tumours and be prognostic. To test this idea, we used a data set of >3,600 clinically annotated and transcriptionally profiled breast cancer samples (Supplementary Table 8) and confirmed that the signature enlisting the validated YAP/TAZ/TEAD direct targets (see Fig. 2b) was differentially expressed in G3 and G_1 tumours, and identified tumours with poor prognosis as determined by Kaplan–Meier analyses (Fig. 3e,f). Moreover, the signature of direct targets statistically correlates with the expression of independent YAP/TAZ signatures, and with the levels of *TAZ* messenger RNA, which is amplified in a subset of breast tumours[16,19] (Supplementary Fig. 3i). Thus, the expression of direct YAP/TAZ/TEAD target genes here identified correlates with YAP/TAZ activation in human tumours.

Genomic co-occupancy of AP-1 and YAP/TAZ/TEAD

De novo motif analyses in YAP/TAZ/TEAD peaks revealed that, after TEAD consensus, the second most frequent motif corresponded to the consensus for AP-1 transcription factors (Supplementary Table 1). AP-1 are dimers of JUN (JUN, JUNB, JUND) and FOS (FOS, FOSB, FOSL1 and FOSL2) families of leucine-zipper proteins[20]. Many of these factors are archetypal oncogenes involved in the control of cellular growth and neoplastic transformation. Most YAP/TAZ/TEAD peaks (70%) contained both a TEAD and an AP-1 motif, with a median distance of about 60 bp.

We next verified that AP-1 factors are indeed recruited to the same genomic regions bound by YAP/TAZ/TEAD4. For this, we considered JUN as a surrogate mark for bound AP-1 dimers, because it is a common component of JUN/FOS and JUN/JUN dimers[20]. By ChIP-seq we identified >24,000 JUN-binding sites. JUN was present in 78% of YAP/TAZ/TEAD-binding sites (4,306/5,522; Fig. 4a,b), and 93% of these shared binding sites are located on active enhancers. This is in line with the notion that composite TEAD and AP-1 motifs dominate the YAP/TAZ cistrome.

JUN peaks were detected on the regulatory regions of well-established YAP/TAZ/TEAD target genes (*CTGF* and *ANKRD1*—Supplementary Fig. 4c), and on the enhancers of 85% of the new targets defining the YAP/TAZ/TEAD cell-proliferation program (as in Fig. 4c). We indeed re-validated by ChIP-qPCR the presence of both JUN and FOSL1 in all tested binding sites (Supplementary Fig. 4d,e). By considering ChIP-seq data from the ENCODE project[21], TEAD4 and AP-1 peaks largely overlap in all examined tumour cell lines (Supplementary Fig. 4f,g), indicating that co-occupancy of TEAD and AP-1 transcription factors on the same regions is a widespread phenomenon. To test the possibility that AP-1 proteins and YAP/TAZ can simultaneously co-occupy chromatin, we carried out a sequential ChIP for YAP followed by anti-JUN reChIP at selected loci. The results indicated that both factors co-occupy the same *cis*-regulatory elements at the same time (Fig. 4d).

Given their vicinity on DNA, we tested whether YAP/TAZ, TEAD and AP-1 proteins could physically interact. By *in situ* proximity ligation assay[22], we found YAP and TEAD1 in close proximity with

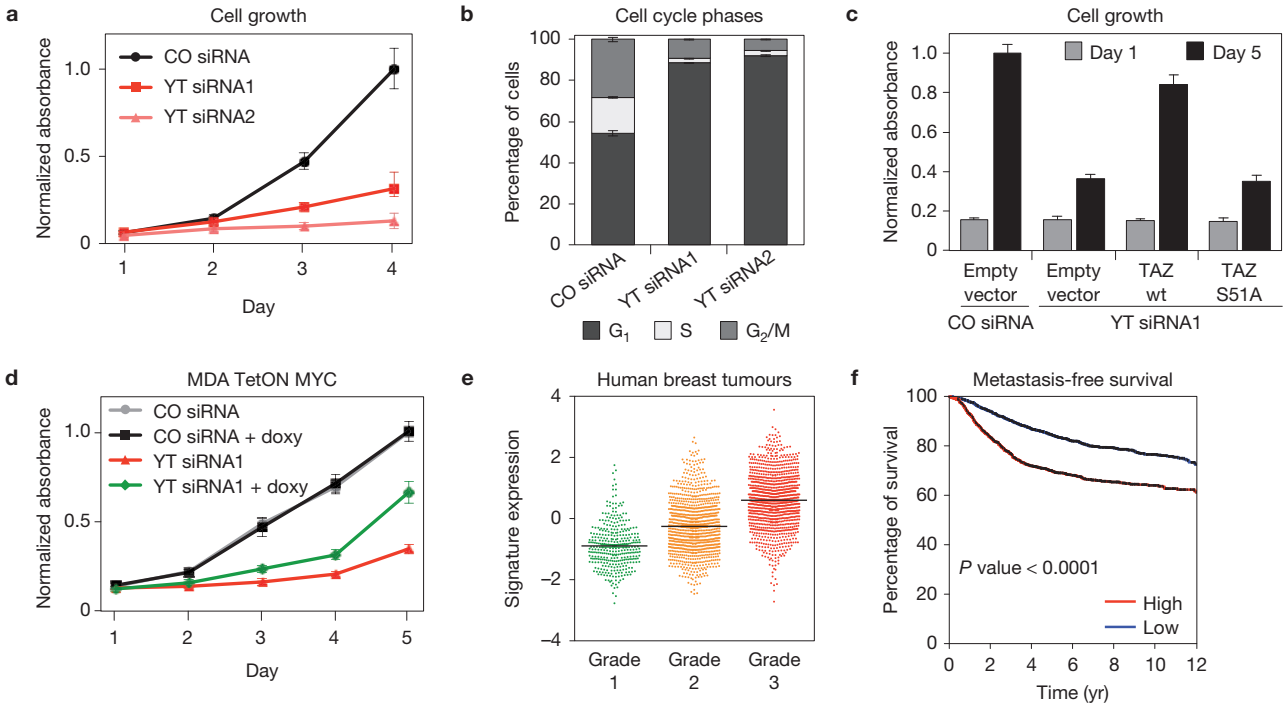

Figure 3 Control of cell proliferation by YAP/TAZ/TEAD. (**a**) Growth curve of MDA-MB-231 cells transfected with control siRNA (CO siRNA) or two different combinations of siRNAs targeting YAP and TAZ (YT siRNA). Data are mean + s.d. of $n=8$ biological replicates. Individual depletion of YAP or TAZ has no effect on cell growth (Supplementary Fig. 3a). (**b**) Percentage of MDA-MB-231 cells in G_1, S and G_2/M phases of cell cycle, as determined by flow-cytometric analysis of DNA content. Cells were transfected with control (CO siRNA) or YAP/TAZ siRNAs (YT siRNA) 48 h before fixation. Data are mean + s.d. of $n=3$ biological replicates. (**c**) Sustained expression of TAZ, but not of TEAD-binding-deficient TAZS51A, rescues cell proliferation in YAP/TAZ-depleted cells. Empty-vector-, wild-type TAZ- (wt) or TAZS51A-transduced MDA-MB-231 cells were transfected with control (CO siRNA) or YAP/TAZ (YT siRNA) siRNAs, as indicated. Proliferation was evaluated as in **f**. Data are mean + s.d. of $n=8$ biological replicates. (**d**) MDA-MB-231 cells were transduced with lentiviral vectors encoding rtTA and doxycycline-inducible MYC (MDA TetON MYC) and transfected with control or YAP/TAZ siRNAs. Where indicated, MYC expression was induced with 0.1 μg ml^{-1} doxycycline at the time of transfection. Cell growth was evaluated as in **f**. Data are mean + s.d. of $n=8$ biological replicates. A control experiment with doxycycline-inducible EGFP is shown in Supplementary Fig. 3h. (**e**) Average gene expression values of validated YAP/TAZ/TEAD direct target genes (listed in Fig. 2b) in invasive breast cancer samples, classified according to their histological grade. Individual data points ($n=3,661$ patient samples) and the mean value (black line) of each group are shown. (**f**) Kaplan–Meier graph representing the probability of cumulative metastasis-free survival in breast cancer patients stratified according to the expression of validated YAP/TAZ/TEAD direct target gene signature. High expression of the signature is associated with shorter metastasis-free survival (log-rank P value < 0.0001). See Methods for reproducibility of experiments.

AP-1 proteins (JUN, FOSL1, JUND) in the nuclei of MDA-MB-231 cells (Fig. 4e). Similar results were obtained in A549 and HCT116 cells (Supplementary Fig. 5b). These interactions were confirmed at the biochemical level: endogenous FOSL1, JUN and JUND robustly co-immunoprecipitated with Flag-tagged TEAD1 (Fig. 4f). Finally, endogenous TEAD1 was co-purified with endogenous FOSL1 and JUND (Fig. 4g,h and Supplementary Fig. 5c).

It has been recently reported that FOS tethers YAP to the promoter of vimentin, leading to a model in which FOS may directly recruit YAP/TAZ on DNA independently of TEAD (ref. 23). By co-immunoprecipitation, we have been unable to detect any protein–protein interaction between YAP/TAZ and the main AP-1 factors expressed in MDA-MB-231, that is, JUN, JUND and FOSL1 (Supplementary Fig. 5d–f). By ChIP-seq, the signal of YAP/TAZ peaks, which matched the TEAD signal, did not correlate with that one of JUN (Supplementary Fig. 5g). Finally, we monitored the capacity of YAP to activate a luciferase reporter containing polymerized TEAD-binding sites (8xGT–LUX) or AP-1-binding sites. Despite being artificial, these reporters are highly specific and sensitive, and allow evaluation of the contribution of individual transcription factors in the absence of other, and potentially confounding, binding sites (a risk of natural promoters). YAP could activate 8xGT–LUX but not the AP-1 sensor (which instead was activated by treatment with the phorbol ester TPA, an established inducer of AP-1; Supplementary Fig. 5h,i). Collectively, our results argue against the possibility that AP-1 dimers mediate YAP/TAZ binding to DNA; that said, it remains possible that, in certain contexts, AP-1 factors may also interact with YAP/TAZ to further enhance the stability of the YAP/TAZ-TEAD and AP-1 complex.

To assess the role of AP-1 in YAP/TAZ/TEAD-mediated transcription, we generated luciferase reporters containing *CTGF* and *ANKRD1* regulatory sequences; both contain motifs for TEAD and AP-1. Mutation of either the TEAD or AP-1 motif reduces luciferase activity (Fig. 4i), indicating that both sites are required to mediate YAP/TAZ-dependent transcription. Taken together, the data indicate that, at YAP/TAZ-bound *cis*-regulatory elements, YAP/TAZ/TEAD and AP-1 proteins form a transcription factor complex bound to composite regulatory elements harbouring both TEAD and AP-1 motifs (Fig. 4j), and jointly regulate gene transcription.

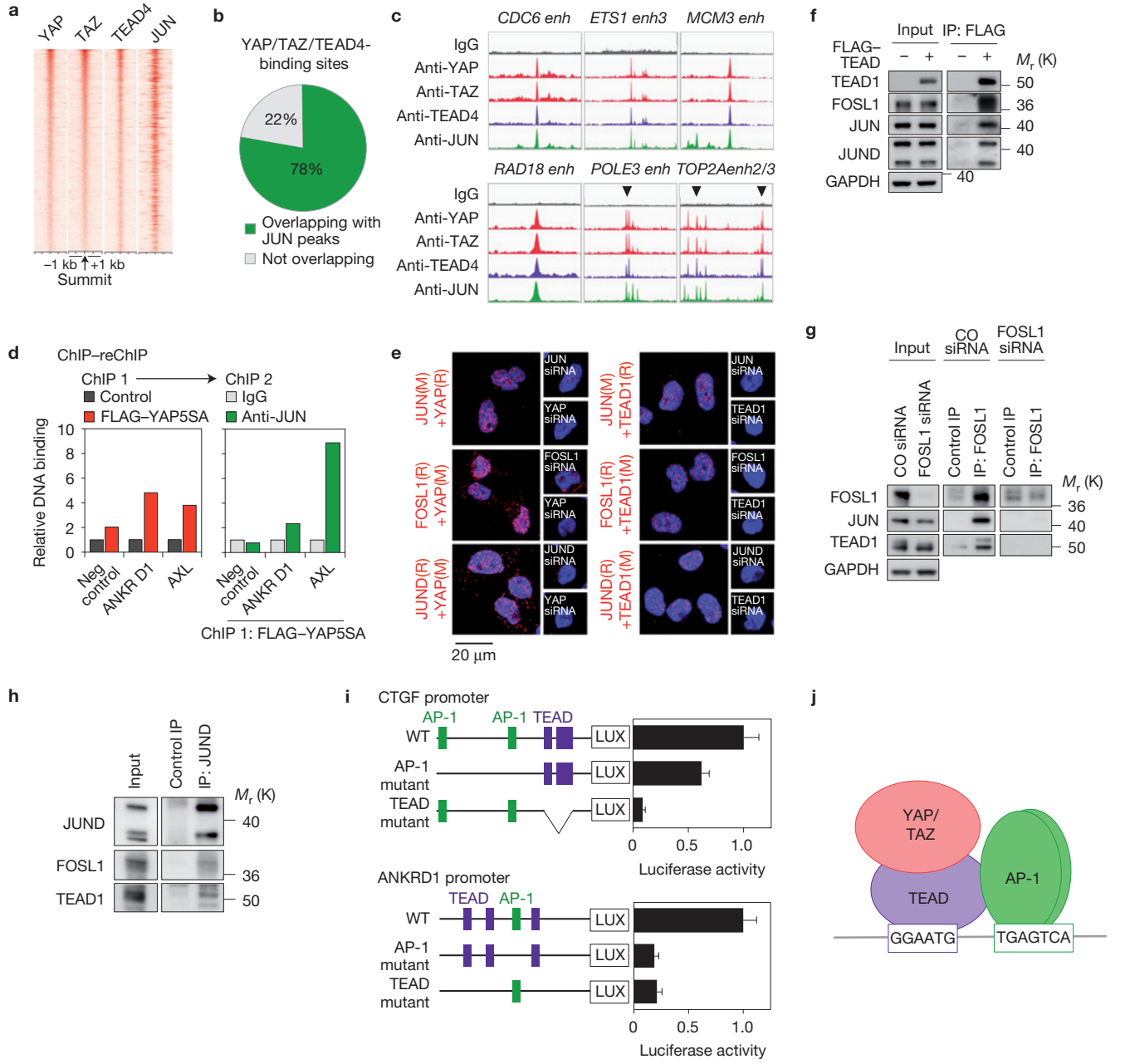

Figure 4 Co-occupancy of YAP/TAZ/TEAD and AP-1 transcription factors at the same genomic loci. (**a**) Density maps of YAP, TAZ, TEAD4 and JUN ChIP-seq reads at YAP/TAZ/TEAD-bound loci. See Supplementary Fig. 4a,b for specificity controls of JUN antibody. (**b**) Percentage of YAP/TAZ/TEAD4 peaks ($n=5,522$) overlapping with JUN ChIP-seq peaks. (**c**) Representative examples of YAP/TAZ/TEAD-bound enhancers co-occupied by JUN in the genome of MDA-MB-231 cells. (**d**) Co-presence of YAP and JUN at the same genomic regions. Results are fold enrichment relative to FLAG IP in control (empty-vector-transduced) cells (ChIP 1) or relative to IgG negative control (ChIP 2). Data from one representative experiment are shown; experiments were repeated twice with similar results. (**e**) *In situ* proximity ligation assay detection of endogenous YAP/AP-1 and TEAD1/AP-1 interactions in MDA-MB-231 cells. Nuclei were counterstained with DAPI (blue). The detected dimers are represented by fluorescent dots (red). The specificity of the interactions is revealed by the reduced number of dots detected after depletion of either of the partners with siRNAs. See Supplementary Fig. 5a for different combinations of antibodies and Supplementary Table 5 for details about antibodies. Magnification is the same for all pictures. (**f**) AP-1 proteins co-precipitate with FLAG–TEAD1 in protein lysates of MDA-MB-231 cells. Input and IP were run on different gels. (**g**) TEAD1 co-precipitates with FOSL1 at endogenous protein levels in MDA-MB-231 cells. IP was performed with FOSL1 (N-17) antibodies. All samples were run on the same gel. JUN is a positive control. (**h**) TEAD1 co-precipitates with JUND at endogenous protein levels in MDA-MB-231 cells. FOSL1 is a positive control. All samples were run on the same gel. (**i**) *CTGF* and *ANKRD1* promoters (either wild-type, or carrying mutations in AP-1- or TEAD-binding sites) were cloned upstream of the luciferase coding sequence and their activity was measured in MDA-MB-231 cells. Data are normalized to wild-type promoter sequences. Data are presented as mean + s.d. of $n=4$ biological replicates from 2 independent experiments. Binding of TEAD and AP-1 proteins to their respective binding sites was verified by DNA pulldown; mutations abolished binding (Supplementary Fig. 5j). (**j**) Model of the complex formed by YAP/TAZ/TEAD and AP-1 on DNA. See Supplementary Fig. 7 for unprocessed original scans of western blots, and Methods for reproducibility of experiments.

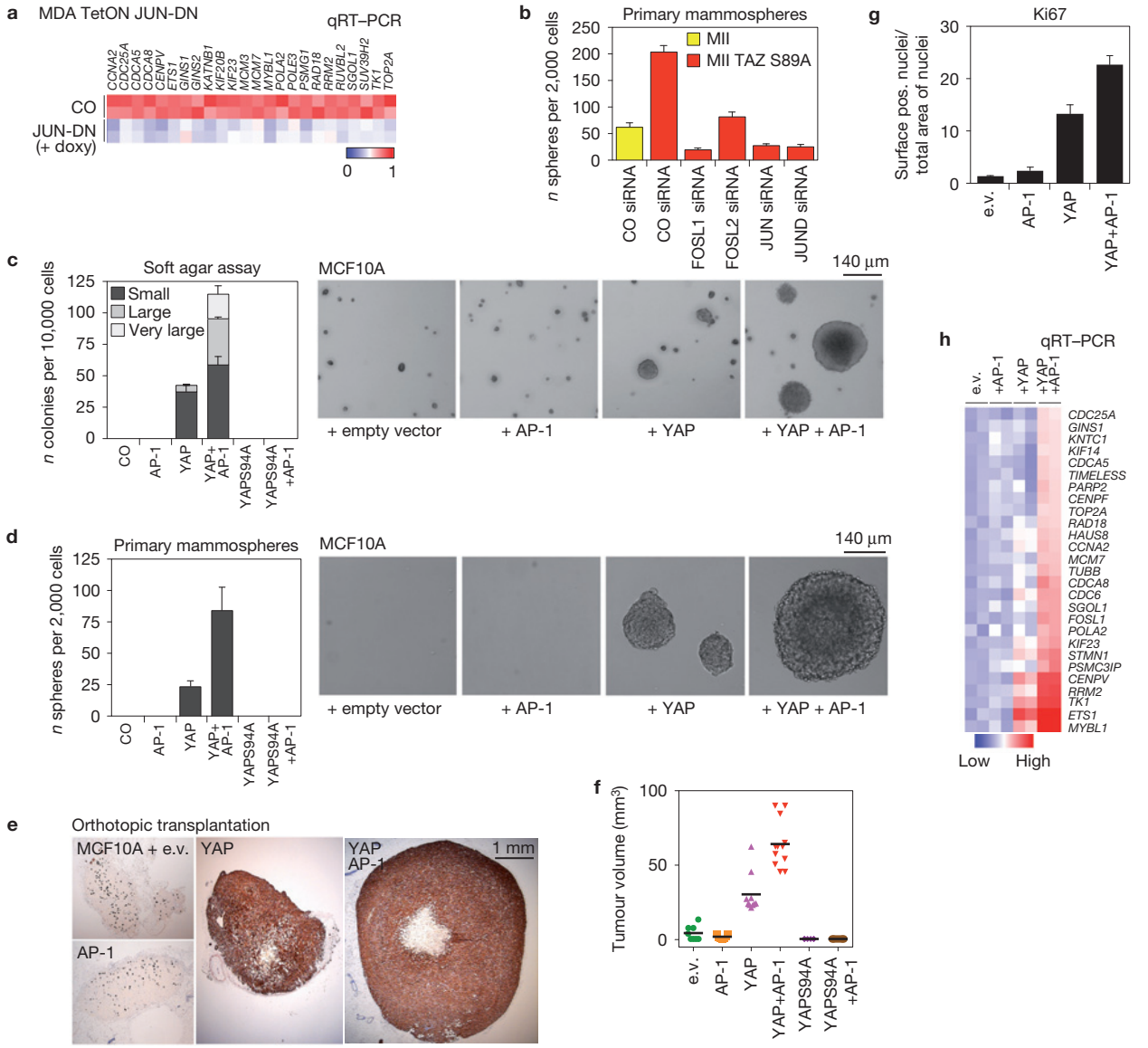

Figure 5 AP-1 factors synergize with YAP/TAZ/TEAD to promote oncogenic growth. (**a**) The expression of YAP/TAZ/TEAD target genes involved in cell growth depends on AP-1. MDA-MB-231 cells were transduced with rtTA and doxycycline-inducible JUN-DN. Cells were left untreated (CO) or treated with 1 µg ml^{-1} doxycycline for 48h. As control, JUN-DN reduces the expression of *FOSL1*, *CTGF* and *ANKRD1* (see Supplementary Fig. 6a). All expression levels are normalized to GAPDH. (**b**) Control and TAZS89A-overexpressing MII cells were transfected with the indicated siRNAs and tested for mammosphere formation. Data are mean + s.d. of $n=6$ biological replicates from a representative experiment. See Supplementary Fig. 6c for a comparison with control MII cells. (**c**) Quantification and representative pictures of colonies formed by the indicated MCF10A derivatives in soft-agar assays. Only background/not growing cell clusters were formed by control and MCF10A+AP-1 cells, and were not counted as colonies. Data are presented as mean + s.d. of $n=3$ biological replicates from a representative experiment. Magnification is the same for all pictures. (**d**) Quantification and representative pictures of primary mammospheres formed by the indicated MCF10A derivatives. Data are presented as mean + s.d. of $n=6$ biological replicates from a representative experiment. Magnification is the same for all pictures. (**e**–**g**) YAP and AP-1 synergize to promote tumour growth. (**e**) Representative immunohistochemistry pictures of xenografts formed by the indicated cell lines. MCF10A cells were stained with a human-specific pan-cytokeratin antibody. (**f**) Tumour volumes at harvesting (individual tumours are plotted, line is the mean; e.v. $n=8$, +AP-1 $n=10$, +YAP $n=10$, +YAP+AP-1 $n=12$, +YAPS94A $n=6$, +YAPS94A+AP-1 $n=6$ tumours). (**g**) Quantification of Ki67-positive cells in tumour sections; data are mean + s.e.m. (e.v. $n=8$, +AP-1 $n=8$, +YAP $n=10$, +YAP+AP-1 $n=11$ tumours). (**h**) YAP5SA and AP-1 cooperate to activate the YAP/TAZ/TEAD proliferative program in MCF10A cells. MCF10A derivatives were grown on a thick Matrigel coating for one week before collection for RNA extraction. mRNA levels of the indicated genes were evaluated by qRT–PCR and normalized to *GAPDH*. See Methods for reproducibility of experiments.

Role of AP-1 in YAP/TAZ-regulated cell growth and tumorigenesis

To verify the requirement of AP-1 proteins for endogenous YAP/TAZ/TEAD target genes, we overexpressed a dominant-negative mutant of JUN (JUN-DN), which allows simultaneous repression of all the AP-1 complexes[24]. Molecularly, expression of JUN-DN reduced transcription of the YAP/TAZ/TEAD cell-proliferation program (Fig. 5a). Functionally, expression of JUN-DN reduced the growth of

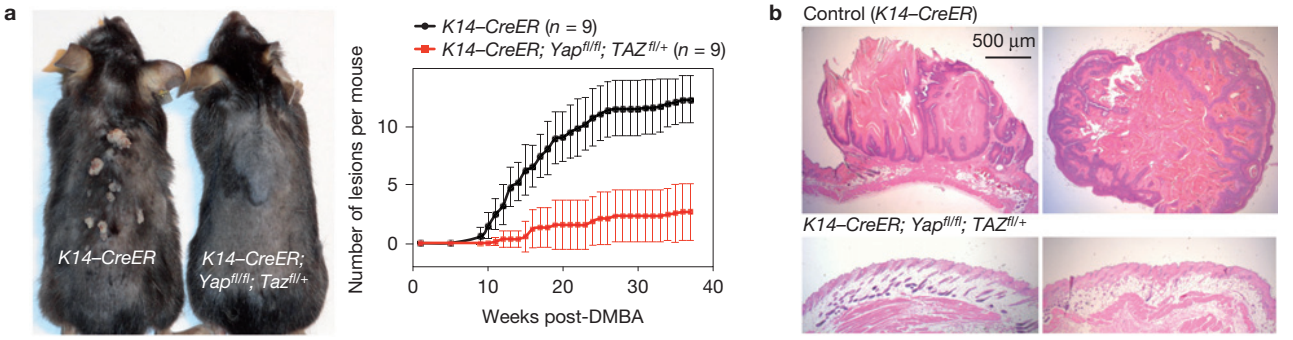

Figure 6 YAP/TAZ are required for AP-1-driven skin tumorigenesis. (**a**) *K14–CreER* and *K14–CreER;Yap$^{fl/fl}$;Taz$^{fl/+}$* mice were treated with tamoxifen to activate Cre in the skin basal layer; after two weeks, mice received a single DMBA administration, followed by repeated TPA treatments for 40 weeks. Left: representative picture of control (*K14–CreER*) and YAP/TAZ-deficient mice at time of collection (40 weeks after the beginning of the experiment). Right: time course of tumour development in mice with the indicated genotypes (data are mean + s.d., $n = 9$ for both experimental groups). See Supplementary Fig. 6d for the verification of Cre-mediated recombination of YAP and TAZ alleles. (**b**) Representative H&E-stained sections of tumours from control mice, or ostensibly normal skin from DMBA/TPA-treated YAP/TAZ conditional knockout mice. Lesions developed by control mice are characterized by skin folds integrated by a core of connective tissue and lined by a hyperplastic, hyperkeratotic, stratified squamous epithelium; some foci of squamous cell carcinoma were also observed (see Supplementary Fig. 6e). Magnification is the same for all pictures. Scale bar is 0.5 mm. See Methods for reproducibility of experiments.

MDA-MB-231 cells, partially phenocopying the effects of YAP/TAZ depletion or TEAD1/2/3/4 depletion (Supplementary Fig. 6b).

The above findings raise the possibility that the oncogenic properties of YAP/TAZ may require AP-1. It has been previously reported that overexpression of TAZ confers 'cancer stem cell' properties to benign MII breast cancer cells[16,25]. We first investigated whether AP-1 factors are involved in these effects. As shown in Fig. 5b, siRNA-mediated depletion of FOSL1, FOSL2, JUN or JUND severely reduced mammosphere formation by MII-TAZS89A cells, indicating that AP-1 factors are essential for these biological activities of TAZ.

Next, we tested whether AP-1 factors are instrumental to enhance YAP/TAZ activity during transformation and oncogenic growth. For this, we transduced immortalized non-tumorigenic mammary epithelial cells (MCF10A) with the following cDNAs: a JUN∼FOSL1 tethered dimer alone[26] (+AP-1 in Fig. 5c–h), YAP5SA alone, or the two constructs together. By monitoring anchorage-independent growth in soft-agar and mammosphere assays, we found that concomitant expression of YAP and the AP-1 dimer strongly enhanced the number and size of colonies when compared with YAP alone (Fig. 5c,d). No colonies were induced by AP-1 alone. Notably, the synergism between YAP and AP-1 requires YAP binding to TEAD, as no soft-agar colonies or mammospheres formed on expression of YAP5SA/S94A (which cannot interact with TEAD), irrespectively of the expression of AP-1 (Fig. 5c,d).

To investigate whether the cooperation between YAP and AP-1 is important for induction of tumorigenic properties, we injected the MCF10A variants described above into the fat-pad of immunocompromised mice. As shown in Fig. 5e–g, expression of AP-1 was per se insufficient to induce tumours, but strongly enhanced the growth of YAP-induced tumours, as indicated by tumour size and Ki67 staining. Mice injected with cells expressing TEAD-binding-deficient YAP instead developed no tumours, irrespectively of the expression of AP-1 dimer (Fig. 5f). Importantly, the functional synergism between AP-1 proteins and YAP/TAZ/TEAD on tumour growth is a mirror of their transcriptional cooperation: although AP-1 dimer alone was insufficient to turn on the YAP/TAZ/TEAD proliferative program, it strongly synergized with YAP to activate transcription of these genes (Fig. 5h). Collectively, results of gain- and loss-of-function assays indicate that AP-1 factors are instrumental for YAP/TAZ transcriptional and biological effects.

Role of YAP/TAZ in AP-1-dependent tumour growth

Having established the relevance of AP-1 for YAP/TAZ-induced cell proliferation and tumour growth, we next asked the converse question, that is, whether YAP/TAZ are important for AP-1-controlled tumorigenesis. To this end, we examined skin tumorigenesis induced by chemical carcinogens. In this model, mutation of H-Ras triggered by a mutagen (DMBA) is per se insufficient for tumour development, requiring cooperation with tumour 'promoters', requiring AP-1 activation. The classic tumour promoter is indeed treatment with phorbol esters (TPA; refs 27,28), well-established triggers of AP-1 activity. In the context of chemical carcinogenesis of the skin, tumour promotion by TPA is blocked by AP-1 inhibition[29]; conversely, TPA treatment can be substituted by gain of AP-1 to fully promote tumour development after DMBA initiation[30]. In line, skin tumours genetically rely on AP-1 activity[11,31,32].

We thus sought to determine whether YAP/TAZ deficiency phenocopies the requirement of AP-1 in tumour promotion. To test this, we treated adult *K14–CreERT2;YAP$^{fl/fl}$;TAZ$^{fl/+}$* mice[33] with tamoxifen to inactivate YAP/TAZ in the skin basal layer; these mice were phenotypically normal, and their epidermis was histologically indistinguishable from wild-type controls (Fig. 6b and Supplementary Fig. 6e). Control and YAP/TAZ-deficient mice were subjected to the chemical carcinogenesis protocol. As shown in Fig. 6a, at 40 weeks all control mice developed papillomas (average 9.3 tumours per mouse, $n = 9$). Strikingly, YAP/TAZ-deficient mice (which still had a normal skin after YAP/TAZ inactivation) developed only rare papillomas (1.5 tumours per mouse, $n = 9$), and 2 mice did not develop any tumours. Histological examination confirmed that control mice mostly developed typical papillomas or, more rarely,

foci of squamous cell carcinomas; in contrast, the treated epidermis of *K14–CreERT2;YAP$^{fl/fl}$;TAZ$^{fl/+}$* mice retained normal morphology (Fig. 6b and Supplementary Fig. 6e). These results complement the above findings on the role of AP-1 for YAP/TAZ-induced tumour growth in mammary cells, and show that YAP/TAZ play a crucial role in the DMBA/TPA model of skin tumorigenesis, thus phenocopying the requirement of AP-1 in chemical carcinogenesis of the skin.

DISCUSSION

By carrying out genome-wide analyses of YAP/TAZ-binding sites in breast cancer cells through ChIP-seq, we found that most (91%) YAP/TAZ-bound *cis*-regulatory regions coincide with enhancer elements, located distant from TSSs. This provides a departure from all previous studies on this topic, so far centred exclusively on promoters[9], allowing us to capture new and essential aspects of YAP/TAZ-mediated transcriptional regulation. By using this list of YAP/TAZ genomic interactions, a map of enhancer–promoter pairs and transcriptomic analyses of YAP/TAZ-dependent genes, we unveiled a complex repertoire of direct YAP/TAZ downstream effectors devoted to the control of cell proliferation, a critical process in most YAP/TAZ-dependent biological events. Many YAP/TAZ targets are proteins directly involved in specific steps of the cell cycle. Of these genes, only one (*CDC6*) was previously proposed as a direct YAP/TAZ target[34]. The program also includes transcription factors, such as MYC, potentially able to amplify the effects of YAP/TAZ. Overall, our work massively extends the previous knowledge on the transcriptional regulation of cell proliferation by YAP/TAZ and highlights yet unexplored aspects of YAP/TAZ biology, as well as a host of new therapeutic targets. The biological significance of these findings is further emphasized by the clinical validity of a signature of YAP/TAZ target genes as a prognostic tool in a large set of breast cancer patients.

The transcriptional responses of YAP/TAZ bear at least superficial similarities with the role of E2F factors: both are required for G_1-to-S transition by directly controlling the molecular engines essential for DNA replication. Indeed, by ChIP-PCR experiments mainly using overexpressed YAP and TEAD it has been recently suggested that YAP/TEAD cooperate with E2F in the regulation of some genes from promoters potentially bearing composite TEAD- and E2F-binding consensuses[34]. However, at the genome-wide level, our data at the endogenous protein level do not favour this model, as the E2F consensus is not enriched at YAP/TAZ/TEAD-bound regions (Supplementary Table 1). That said, the E2F motif is present in a number of promoters of genes here identified in the YAP/TAZ-proliferative program (67%, Supplementary Table 5). Collectively, this raises the intriguing hypothesis that YAP/TAZ/TEAD bound to distant enhancers may cooperate with E2F bound to promoters through chromatin looping, thus possibly explaining the requirement of E2F for YAP-mediated cell proliferation[34]. Future work will be required to dissect this model.

A plethora of DNA-binding platforms have been reported for YAP/TAZ (refs 3,8–11). Our ChIP-seq analyses indicate that TEAD factors are the anchors that tether YAP/TAZ to DNA at the genome-wide level; functionally, TEADs are essential for the execution of the entire YAP/TAZ-dependent cell-proliferation program. Surprisingly, of the various transcription factors proposed to work as YAP/TAZ DNA-binding platforms, only the RUNX1/2 motif exhibits a low albeit significant enrichment in our context (Supplementary Table 1) but it is not preferentially enriched close to the summit of YAP/TAZ peaks; this suggests that, in general, RUNX factors are unlikely to serve as YAP/TAZ DNA-binding platforms.

A key finding of our genome-wide analyses is that AP-1 factors are critical and global regulators of YAP/TAZ/TEAD-dependent gene expression. AP-1 are present in most YAP/TAZ/TEAD-binding sites, forming a transcription factor complex bound to composite regulatory elements harbouring both the TEAD and the AP-1 motifs. AP-1 factors do not mediate YAP/TAZ DNA-recognition, and cannot sustain YAP/TAZ activities in the absence of YAP/TAZ binding to TEAD; instead AP-1 transcription factors strongly support YAP/TAZ/TEAD-dependent gene expression and greatly enhance oncogenic growth triggered by YAP. Conversely, AP-1 inactivation blunts the proliferative and cancer stem cell properties induced by TAZ. It is interesting to note that YAP/TAZ directly activate FOSL1 (Fig. 2b and Supplementary Fig. 2b,c), suggesting a feed-forward/self-enabling loop.

AP-1 factors are classic proto-oncogenes and are important as tumour 'promoters', cooperating with Ras 'initiating' mutations in skin chemical carcinogenesis[27,29,30]. Our findings suggest that part of these attributes could rely on the ability of AP-1 dimers to synergize with YAP/TAZ on chromatin. Supporting this notion, gain-of-AP-1 is per se insufficient to sustain oncogenic growth in the absence of YAP overexpression in mammary epithelial cells. In line, YAP/TAZ are genetically required for skin tumorigenesis on the classical tumour initiation/promotion protocol with DMBA/TPA. That said, further experiments are required to formally demonstrate the transcriptional cooperation between YAP/TAZ/TEAD and AP-1 in skin tumours.

The role of AP-1 proteins as general factors in YAP/TAZ-transcriptional regulation adds a number of new modalities to feed information to the YAP/TAZ genetic program. For example, AP-1 proteins are activated by inflammation and stress inputs[20], and these may sensitize cells to YAP/TAZ-inducing inputs[3]. Then, there is a widely reported implication of AP-1 in epithelial–mesenchymal transition (EMT), especially in breast cancer cells; for example, recent reports have linked high FOSL1 expression to EMT and metastasis[35,36]. Given the established connections between YAP/TAZ and EMT/malignant traits[3], it is thus tempting to speculate that AP-1 factors may cooperate with YAP/TAZ for metastatic dissemination or colonization.

It is also notable that AP-1 are dimers of variable composition, and do not always behave as oncogenes[20], adding further complexity and potentially cell specificity to the effects of YAP/TAZ. Further studies are required to dissect these interplays in distinct biological contexts in which YAP/TAZ and AP-1 have been so far only independently implicated, including cancer, stem cell biology, regeneration and differentiation. □

METHODS

Methods and any associated references are available in the online version of the paper.

Note: Supplementary Information is available in the online version of the paper

ACKNOWLEDGEMENTS

We thank O. Wessely, S. Dupont and G. Martello for comments; M. Morgante and E. Aleo for deep-sequencing (IGA, Udine); V. Guzzardo for histology; D. J. Pan (Johns Hopkins University, Maryland, USA) for gifts of Yap fl/fl mice; D. Metzger and P. Chambon (University of Strasbourg, France) for K14–Cre–ERT2 transgenics; L. Naldini (San Raffaele Scientific Institute, Italy) for lentiviral plasmids and

L. Bakiri (Spanish National Cancer Research Centre (CNIO), Spain) for AP-1 expression constructs. We are grateful to C. Frasson for flow cytometry analyses. We acknowledge a donation in memoriam of L. Simonutti. F.Z. and L.A. are supported by a fellowship from the Italian Association for Cancer Research (AIRC). M.F. is supported by an assistant professorship from FIRB Accordi di Programma 2011 RBAP11T3WB. This work is supported by AIRC-MFAG to M.C.; from AIRC Special Program Molecular Clinical Oncology '5 per mille' to S.P. and S.B.; Epigenetics Flagship project CNR-MIUR grants to S.B. and S.P.; AIRC-IG Grant to S.P. Work in the laboratory of S.P. is also supported by ERC-2014-ADG.

AUTHOR CONTRIBUTIONS

F.Z. and G.B. performed experiments, M.F., M.C. and S.B. performed bioinformatic analysis, E.Q. helped with molecular biology, L.A. and A.R. performed *in vivo* experiments, B.B. helped with ChIP and 3C protocols, M.C. and S.P. planned, discussed and organized the work and wrote the manuscript.

COMPETING FINANCIAL INTERESTS

The authors declare no competing financial interests.

Published online at http://dx.doi.org/10.1038/ncb3216
Reprints and permissions information is available online at www.nature.com/reprints

1. Sudol, M. Yes-associated protein (YAP65) is a proline-rich phosphoprotein that binds to the SH3 domain of the Yes proto-oncogene product. *Oncogene* **9,** 2145–2152 (1994).
2. Kanai, F. *et al.* TAZ: a novel transcriptional co-activator regulated by interactions with 14-3-3 and PDZ domain proteins. *EMBO J.* **19,** 6778–6791 (2000).
3. Piccolo, S., Dupont, S. & Cordenonsi, M. The biology of YAP/TAZ: hippo signaling and beyond. *Physiol. Rev.* **94,** 1287–1312 (2014).
4. Ramos, A. & Camargo, F. D. The Hippo signaling pathway and stem cell biology. *Trends Cell Biol.* **22,** 339–346 (2012).
5. Harvey, K. F., Zhang, X. & Thomas, D. M. The Hippo pathway and human cancer. *Nat. Rev. Cancer* **13,** 246–257 (2013).
6. Halder, G. & Johnson, R. L. Hippo signaling: growth control and beyond. *Development* **138,** 9–22 (2011).
7. Aragona, M. *et al.* A mechanical checkpoint controls multicellular growth through YAP/TAZ regulation by actin-processing factors. *Cell* **154,** 1047–1059 (2013).
8. Strano, S. *et al.* The transcriptional coactivator Yes-associated protein drives p73 gene-target specificity in response to DNA damage. *Mol. Cell* **18,** 447–459 (2005).
9. Zhao, B. *et al.* TEAD mediates YAP-dependent gene induction and growth control. *Genes Dev.* **22,** 1962–1971 (2008).
10. Rosenbluh, J. *et al.* β-Catenin-driven cancers require a YAP1 transcriptional complex for survival and tumorigenesis. *Cell* **151,** 1457–1473 (2012).
11. Yagi, R., Chen, L. F., Shigesada, K., Murakami, Y. & Ito, Y. A WW domain-containing yes-associated protein (YAP) is a novel transcriptional co-activator. *EMBO J.* **18,** 2551–2562 (1999).
12. Calo, E. & Wysocka, J. Modification of enhancer chromatin: what, how, and why? *Mol. Cell* **49,** 825–837 (2013).
13. Rhie, S. *et al.* Nucleosome positioning and histone modifications define relationships between regulatory elements and nearby gene expression in breast epithelial cells. *BMC Genomics* **15,** 331 (2014).
14. Jin, F. *et al.* A high-resolution map of the three-dimensional chromatin interactome in human cells. *Nature* **503,** 290–294 (2013).
15. Rao, S. S. *et al.* A 3D map of the human genome at kilobase resolution reveals principles of chromatin looping. *Cell* **159,** 1665–1680 (2014).
16. Cordenonsi, M. *et al.* The Hippo transducer TAZ confers cancer stem cell-related traits on breast cancer cells. *Cell* **147,** 759–772 (2011).
17. Bhat, K. P. *et al.* The transcriptional coactivator TAZ regulates mesenchymal differentiation in malignant glioma. *Genes Dev.* **25,** 2594–2609 (2011).
18. Lamar, J. M. *et al.* The Hippo pathway target, YAP, promotes metastasis through its TEAD-interaction domain. *Proc. Natl Acad. Sci. USA* **109,** E2441–E2450 (2012).
19. Skibinski, A. *et al.* The Hippo transducer TAZ interacts with the SWI/SNF complex to regulate breast epithelial lineage commitment. *Cell Rep.* **6,** 1059–1072 (2014).
20. Eferl, R. & Wagner, E. F. AP-1: a double-edged sword in tumorigenesis. *Nat. Rev. Cancer* **3,** 859–868 (2003).
21. E. P. Consortium, An integrated encyclopedia of DNA elements in the human genome. *Nature* **489,** 57–74 (2012).
22. Koos, B. *et al.* Analysis of protein interactions *in situ* by proximity ligation assays. *Curr. Top. Microbiol. Immunol.* **377,** 111–126 (2014).
23. Shao, D. D. *et al.* KRAS and YAP1 converge to regulate EMT and tumor survival. *Cell* **158,** 171–184 (2014).
24. Brown, P. H., Alani, R., Preis, L. H., Szabo, E. & Birrer, M. J. Suppression of oncogene-induced transformation by a deletion mutant of c-jun. *Oncogene* **8,** 877–886 (1993).
25. Santner, S. J. *et al.* Malignant MCF10CA1 cell lines derived from premalignant human breast epithelial MCF10AT cells. *Breast Cancer Res. Treat.* **65,** 101–110 (2001).
26. Bakiri, L., Matsuo, K., Wisniewska, M., Wagner, E. F. & Yaniv, M. Promoter specificity and biological activity of tethered AP-1 dimers. *Mol. Cell Biol.* **22,** 4952–4964 (2002).
27. Balmain, A. & Yuspa, S. H. Milestones in skin carcinogenesis: the biology of multistage carcinogenesis. *J. Invest. Dermatol.* **134,** E2–E7 (2014).
28. Bailleul, B. *et al.* Skin hyperkeratosis and papilloma formation in transgenic mice expressing a ras oncogene from a suprabasal keratin promoter. *Cell* **62,** 697–708 (1990).
29. Young, M. R. *et al.* Transgenic mice demonstrate AP-1 (activator protein-1) transactivation is required for tumor promotion. *Proc. Natl Acad. Sci. USA* **96,** 9827–9832 (1999).
30. Briso, E. M. *et al.* Inflammation-mediated skin tumorigenesis induced by epidermal c-Fos. *Genes Dev.* **27,** 1959–1973 (2013).
31. Zenz, R. *et al.* c-Jun regulates eyelid closure and skin tumor development through EGFR signaling. *Dev. Cell* **4,** 879–889 (2003).
32. Chen, Y. & Lai, M. Z. c-Jun NH2-terminal kinase activation leads to a FADD-dependent but Fas ligand-independent cell death in Jurkat T cells. *J. Biol. Chem.* **276,** 8350–8357 (2001).
33. Azzolin, L. *et al.* YAP/TAZ incorporation in the beta-catenin destruction complex orchestrates the Wnt response. *Cell* **158,** 157–170 (2014).
34. Kapoor, A. *et al.* Yap1 activation enables bypass of oncogenic Kras addiction in pancreatic cancer. *Cell* **158,** 185–197 (2014).
35. Tam, W. L. *et al.* Protein kinase C alpha is a central signaling node and therapeutic target for breast cancer stem cells. *Cancer Cell* **24,** 347–364 (2013).
36. Bakiri, L. *et al.* Fra-1/AP-1 induces EMT in mammary epithelial cells by modulating Zeb1/2 and TGFbeta expression. *Cell Death Differ.* **22,** 336–350 (2015).

DOI: 10.1038/ncb3216

METHODS

Plasmids. pCS2-FLAG-mTAZ, pBABE-hygro-FLAG-mTAZ wt and S89A, pCDNA-FLAG-YAP, FU-tet-o-EGFP-ires-PURO, and 8xGTIIC–LUX were previously described[7,16,33,37] TAZS51A and YAPS94A were generated by PCR-mediated mutagenesis and cloned into pBABE retroviral vectors. pCMV6-FLAG-MYC-TEAD1 was from Origene. FU-tet-o-hc-myc (no. 19775, ref. 38) and FUdeltaGW-rtTA (no. 19780, ref. 38) were purchased from Addgene. pBABE-puro-JUN∼FOSL1-FLAG was a gift from L. Bakiri[26]. Doxycycline-inducible JUN-DN lentiviral construct was obtained by substituting the Oct4 sequence in FUW-tetO-hOCT4 (Addgene no. 20726) with JUN-DN cDNA from pMIEG3-JunDN (Addgene no. 40350). pAP1-luc was from Clontech and pRL-TK from Promega. CTGF and ANKRD1 luciferase reporters were generated by amplifying CTGF (hg19, chr6:132272417-132273191)/ANKRD1(chr10:92680870-92681128) promoters by PCR from genomic DNA and cloning into pGL3 basic; for AP-1 mutants, point mutations were introduced by PCR in AP-1-binding sites; for TEAD mutants, a single deletion comprising the three TEAD-binding sites was introduced in CTGF promoter, whereas point mutations were generated in the ANKRD1 promoter. All constructs were confirmed by sequencing.

Cell lines and transfections. MDA-MB-231, A549 and HCT116 cells were from ICLC; MCF10A and HEK293 cells were from ATCC. MII cells were a gift from F. R. Miller[25] (Karmanos Cancer Institute, USA). MDA-MB-231 cells were authenticated by DNA profiling of highly polymorphic STR loci. All cell lines were routinely tested for mycoplasma contamination and were negative. None of the cell lines used in this study is present in the database of commonly misidentified cell lines. A549 cells were cultured in DMEM/F12 (Life Technologies) supplemented with 10% FBS, glutamine and antibiotics; culture conditions for all of the other cell lines were as previously described[16,39].

siRNAs were transfected with Lipofectamine RNAi-MAX (Life Technologies), and DNA transfections were performed with TransitLT1 (Mirus Bio) according to the manufacturer's instructions. Cells were collected 48 h after transfection, unless differently specified. Sequences of siRNAs are provided in Supplementary Table 9. Retroviral and lentiviral infections were carried out as in refs 40,41. MCF10A e.v. cells were infected with pBABE-puro and pBABE-blasti empty vectors; MCF10A+AP-1 were infected with pBABE-puro-JUN∼FOSL1-FLAG and pBABE-blasti empty vector; MCF10A+YAP (or 5SA/S94A) were infected with pBABE-puro empty vector and pBABE-blasti-FLAG-YAP5SA (or 5SA/S94A); MCF10A+YAP+AP-1 were infected with pBABE-puro-JUN∼FOSL1-FLAG and pBABE-blasti-FLAG-YAP5SA (or 5SA/S94A).

ChIP-seq, ChIP-qPCR and ChIP-reChIP. Chromatin immunoprecipitation was performed as described in ref. 42 Antibodies are listed in Supplementary Table 6. Briefly, cells were crosslinked with 1% formaldehyde (Sigma) in culture medium for 10 min at room temperature, and chromatin from lysed nuclei was sheared to 200–600 bp fragments using a Branson Sonifier 450A. For ChIP-seq, ∼200 μg of chromatin was incubated with 10 μg of antibody overnight at 4 °C. Antibody/antigen complexes were recovered with ProteinA-Dynabeads (Invitrogen) for 2 h at 4 °C. ChIP'd DNA from 3 immunoprecipitations was pooled to generate libraries with the Ovation Ultra Low Library Prep Kit (NuGEN) according to the manufacturer's instructions. Sequencing was performed on an Illumina HiSeq 2500 platform.

For ChIP-qPCR, ∼100 μg of sheared chromatin and 3–5 μg of antibody were used. For ChIPs of modified histones, at least 50 μg of chromatin was incubated with 2 μg of antibody. Quantitative real-time PCR was carried out with a Rotor-Gene Q (Qiagen) thermal cycler; each sample was analysed in triplicate. The amount of immunoprecipitated DNA in each sample was determined as the fraction of the input (amplification efficiency^(Ct INPUT–Ct ChIP)), and normalized to the IgG control. Primers are listed in Supplementary Table 9.

For ChIP-reChIP, MDA-MB-231 cells stably expressing FLAG–YAP5SA were used. Chromatin was incubated with anti-FLAG magnetic beads (Sigma) for 4 h at 4 °C; after washing, immunocomplexes were eluted by incubating beads in lysis buffer 3 + 0.5 μg μl^{-1} 3× FLAG peptide (Sigma) for 1 h at 4 °C; two sequential elutions were performed. Eluted chromatin was diluted 1:3 with lysis buffer 3, supplemented with 1% Triton X-100 and incubated with 3 μg of normal mouse IgG or anti-JUN antibody, overnight at 4 °C.

Peak calling and data analysis. Raw reads were aligned using Bowtie (version 0.12.7; ref. 43) to build version hg19 of the human genome retaining only uniquely mapped reads. Redundant reads were removed using SAMtools. The IDR (Irreproducible Discovery Rate) framework[44] was used to assess the consistency of replicate experiments and to obtain a high-confidence single set of peak calls for each transcription factor as described in the ChIP-seq guidelines of the ENCODE consortium[45]. MACS2 version 2.0.10 (ref. 46) was used to call peaks in individual replicates using IgG ChIP-seq as the control sample and an IDR threshold of 0.01 was applied for all data sets to identify an optimal number of peaks.

Normalized read density (reads per million, rpm) was calculated from pooled replicates using the MACS2 callpeak function and displayed using the Integrative Genomics Viewer (IGV).

Heatmaps were generated using a custom R script that considers a 2-kb window centred on peak summits and calculates the normalized read density with a resolution of 50 bp.

The genomic location of the peaks and their distance to the TSS of annotated genes were calculated using the annotatePeakInBatch function of the ChIPpeakanno R package and GENCODE annotation version 16 (ref. 47). Only genes classified as protein coding and with status equal to KNOWN were considered.

The findOverlappingPeaks function of the same package was used with default parameters to identify overlapping peaks and calculate the distance between their summits. TAZ peak coordinates and summit positions were used to represent common peaks between YAP and TAZ peaks (YAP/TAZ peaks) and were used when comparing YAP/TAZ peaks with other ChIP-seq data.

Definition of MDA-MB-231 promoters and enhancers. Raw reads for ChIP-seq data of histone modifications (H3K4me1, H3K4me3 and H3K27ac) in MDA-MB-231 (ref. 13) were downloaded from SRA (SRP028597) and aligned using Bowtie version 0.12.9 to build version hg19 of the human genome retaining only uniquely mapped reads. Redundant reads were removed using SAMtools. Peak calls and read density tracks were generated using SPP version 1.11 (ref. 48) with default parameters and using as the control sample the IgG ChIP-seq data generated in our laboratory because of the low sequencing depth of the input DNA contained in SRP028597.

The distance between histone modification peaks and the transcription start sites (TSSs) of protein-coding genes (GENCODE v. 16 and REFSEQ annotations), and the overlap between histone mark peaks were calculated as previously described for transcription factor peaks.

The presence of H3K4me1 and H3K4me3 peaks, their genomic locations and their overlap were the criteria used to define promoters and enhancers: H3K4me3 peaks not overlapping with H3K4me1 peaks and close to a TSS (±5 kb) were defined as promoters, as NA otherwise; H3K4me1 peaks not overlapping with H3K4me3 peaks were defined as enhancers; regions with the co-presence of H3K4me1 and H3K4me3 peaks were visually inspected on IGV and were defined as promoters, enhancers or NA after the evaluation of the proximity to a TSS and the comparison of the enrichment signals. Finally, promoters or enhancers were defined as active if overlapping with H3K27ac peaks.

YAP/TAZ/TEAD peak annotation. YAP/TAZ/TEAD peaks were annotated as promoters or enhancers if their summit was overlapping with promoter or enhancer regions as defined above. Peaks with the summit falling in regions with no H3K4me1 or H3K4me3 peaks, or in NA regions were defined as 'not assigned' and discarded from subsequent analyses.

YAP/TAZ/TEAD peak summits were compared with FAIRE peaks using the list downloaded from GSE49651.

YAP/TAZ/TEAD peaks falling on promoters were assigned to the closest TSS. YAP/TAZ/TEAD peaks falling on active enhancers were annotated using the chromatin interactions reported in Supplementary data 2 of ref. 14, derived from a high-resolution Hi-C experiment; the data sheets report the genomic locations of all target peaks interacting with more than 10,000 anchors located at gene promoters. YAP/TAZ peaks overlapping with these target peaks were assigned to the corresponding interacting promoter region. Finally, YAP/TAZ/TEAD peaks falling on inactive enhancers were not assigned to targets.

Motif discovery in ChIP-seq peaks. *De novo* motif discovery was performed with the findMotifsGenome function of Homer software[49]. Motifs were searched in 500 bp windows centred at the peak summits. Occurrences of *de novo* and known motifs inside the peaks were found using the annotatePeaks function of the same software. Known motifs were retrieved from the Homer motif database and from the JASPAR database (http://jaspar.genereg.net).

Gene expression analysis by Affymetrix microarrays. MDA-MB-231 cells were transfected with control or two independent combinations of YAP/TAZ siRNAs for 48 h; four biological replicates for each sample were prepared. Transcriptomic data were obtained using Affymetrix GeneChips Human Genome U133 Plus 2.0. Raw data were as in ref. 50, but analysed as detailed below.

Microarray analyses were performed in R (version 2.15.1). Probe level signals were converted to expression values using the robust multi-array average procedure RMA (ref. 51) of the Bioconductor affy package and a custom chip definition file based on the Entrez gene database (version 17, ref. 52). Differentially expressed genes were identified using the Significance Analysis of Microarray algorithm coded in the samr R package[53]. In SAM, we estimated the percentage of false positive predictions

(that is, false discovery rate, FDR) with 100 permutations. To identify genes regulated by YAP/TAZ, we selected those genes coherently downregulated with a FDR $\leq 0.1\%$ in both silencing experiments, and present in GENCODE v.16 annotation. This selection resulted in 1,534 downregulated genes. These genes were compared with the list of candidate YAP/TAZ direct target genes described above. As a result, 379 genes were defined as YAP/TAZ direct positive targets, as they were downregulated by YAP/TAZ depletion and associated with at least one YAP/TAZ peak.

Gene ontology analysis. Gene Ontology (GO) analyses were performed using DAVID (ref. 54). The full list of GO terms of the Biological Process category enriched in direct positive YAP/TAZ targets is presented in Supplementary Table 4. GO terms with a Benjamini–Hochberg FDR $\leq 5\%$ were considered significantly enriched. GO terms significantly enriched among YAP/TAZ/TEAD direct positive target genes could be assigned to two broad categories: 'cell proliferation' and 'RNA metabolism and transport' (Supplementary Table 4).

Promoters of the genes involved in cell proliferation were defined as 1,000 bp windows centred at the TSS. *De novo* motif discovery and occurrence of known motifs were performed as described above. Used known motifs are E2F4(E2F) from the Homer motif database and (MA0024.1) for E2F1 from the JASPAR database.

Analysis of public ChIP-seq data. ChIP-seq data sets for transcription factors and histone modifications that were reanalysed in this study are listed in Supplementary Table 7.

For data of the ENCODE project[21], aligned reads and peak calls were downloaded from the ENCODE project repository. When available, transcription factor peaks uniformly generated by the ENCODE Analysis Working Group (available at http://hgdownload.cse.ucsc.edu/goldenPath/hg19/encodeDCC/wgEncodeAwgTfbsUniform) were used. Otherwise, aligned reads and peak calls of the first replicate were used. Genomic annotation of TEAD4 or TEAD1 peaks and overlap between peaks were calculated as described for ChIP-seq data of MDA-MB-231 cells.

Gene expression analysis. MDA-MB-231 cells were transfected with siRNAs (or treated with doxycycline) 48 h before collection. RNA extraction was performed with RNeasy Mini Kit (QIAGEN). MCF10A cells were cultured as spheres on a thick coating of gelled Matrigel for 8 days (described in ref. 55); cells were recovered with BD Cell Recovery Solution (BD Biosciences), and collected in Trizol (Invitrogen) for total RNA extraction.

Reverse transcription and qPCR were performed as described in ref. 7. Expression levels are normalized to GAPDH. Primers are listed in Supplementary Table 9. For the experiments in Figs 2b and 5a,h cDNA was synthesized with the High Capacity RNA-to-cDNA Kit (Invitrogen) and target genes were quantified with custom TaqMan Low Density Arrays on a 7900HT Fast Real-Time PCR System (Applied Biosystems), using TaqMan Universal PCR Master Mix (Applied Biosystems). TaqMan assays included in the array are listed in Supplementary Table 9. Expression levels are normalized to GAPDH.

Chromatin conformation capture (3C). 3C was performed as described in ref. 56 with some modifications. Adherent cells were incubated with a solution containing 1.5% formaldehyde for 10 min at room temperature, followed by 5 min treatment with 0.125 M glycine/PBS. Cells were incubated with 0.05% trypsin for 10 min at 37 °C, before completely detaching them with a cell scraper. Collected cells were pelletted, washed in PBS and incubated with lysis buffer for 15 min at 4 °C. Nuclei were digested with HindIII restriction enzyme (NEB), and highly diluted digested chromatin was ligated with T4 DNA ligase (NEB). De-crosslinked DNA fragments were purified by phenol–chloroform extraction and ethanol precipitation. A reference template was generated by digesting, mixing and ligating bacterial artificial chromosomes spanning the genomic regions of interest. 3C templates and the reference template were used to perform semiquantitative PCR with GO Taq G2 Flexi DNA Polymerase (Promega). Primers flanked the HindIII restriction sites located close to MYC and TOP2A promoters (anchors) and enhancers (primer sequences are provided in Supplementary Table 9). Data are presented as the ratio of amplification obtained with 3C templates from MDA-MB-231 cells and with the reference template. PCR performed on control 3C template obtained from not-crosslinked cells never yielded any product. PCR products were verified by sequencing.

Collection and processing of breast cancer gene expression data. We started from a collection of 4,640 samples from 27 major data sets comprising microarray data of breast cancer samples annotated with histological tumour grade and clinical outcome (Supplementary Table 8). The collection was normalized and annotated with clinical information as described in ref. 50. This resulted in a compendium (meta-data set) comprising 3,661 unique samples from 25 independent cohorts (Supplementary Table 8).

Survival analysis. To identify two groups of tumours with either high or low YAP/TAZ/TEAD direct target gene signature we used the classifier described in ref. 55, that is, a classification rule based on the YAP/TAZ/TEAD direct target gene signature score. Tumours were classified as 'YAP/TAZ/TEAD direct target gene signature' Low if the combined score was negative and as 'YAP/TAZ/TEAD direct target gene signature' High if the combined score was positive. To evaluate the prognostic value of the signature, we estimated, using the Kaplan–Meier method, the probabilities that patients would remain free of metastasis. The Kaplan–Meier curves were compared using the log-rank (Mantel–Cox) test. P values were calculated according to the standard normal asymptotic distribution. Survival analysis was performed in GraphPad Prism.

Average signature expression and correlation. Average signature expression has been calculated as the standardized average expression of all signature genes in sample subgroups. To test the association between YAP/TAZ/TEAD direct target gene signature, *TAZ* (*WWTR1*) expression level, and YAP/TAZ signatures[37,57], we calculated the Pearson's product moment correlation coefficient using the *cor.test* function of the *stat* R package.

Co-immunoprecipitation assays and DNA pulldown. For immunoprecipitation of FLAG-tagged proteins, MDA-MB-231 cells were transfected with 80 ng cm^{-2} of FLAG–TEAD1, FLAG–YAP or FLAG–TAZ plasmids. DNA amount was adjusted to 160 ng cm^{-2} with pBluescript. For immunoprecipitation of endogenous proteins, MDA-MB-231 and HCT116 cells were transfected with siRNAs as indicated. Cells were collected 48 h after transfection. Cell lysis and immunoprecipitation were performed as in ref. 33. DNA pulldown was performed as in ref. 16.

Western blot. Whole-cell lysates were obtained by sonication in lysis buffer (20 mM HEPES (pH 7.8), 100 mM NaCl, 5% glycerol, 5 mM EDTA, 0.5% Np40, and protease and phosphatase inhibitors). The western blot procedure was carried out as described in ref. 39. Primary antibodies are listed in Supplementary Table 6.

***In situ* proximity ligation assay.** *In situ* PLA was performed with DuoLink In Situ Reagents from Olink Bioscience (Sigma). MDA-MB-231 cells were transfected with siRNAs in standard cell culture dishes, seeded in fibronectin-coated glass chamber slides 24 h later, and fixed in 4% PFA for 10 min at room temperature 48 h after transfection. Proximity ligation assays were performed as indicated by the provider's protocol, after an overnight incubation with primary antibodies following the immunofluorescence protocol described in ref. 37. Images were acquired with a Leica SP5 confocal microscope equipped with a CCD camera; for each field, a Z-stack was acquired; images were processed using Volocity software (PerkinElmer). Primary antibodies are listed in Supplementary Table 6.

Luciferase reporter assays. TEAD reporter (8xGTIIC–LUX; ref. 37) and AP-1 reporter (pAP1-luc, Clontech; 25 ng cm^{-2}) were transfected into HEK293 cells, together with increasing doses of pCDNA-FLAG-YAPwt (1.25, 2.5, 6.25 and 12.5 ng cm^{-2}) and TK-Renilla (25 ng cm^{-2}) to normalize for transfection efficiency. CTGF and ANKRD1 luciferase constructs were co-transfected with pRL-TK in MDA-MB-231 cells (75 ng cm^{-2}). DNA content in all samples was kept uniform by adding pBluescript plasmid up to 250 ng cm^{-2}. Where indicated, 2 nM TPA was added 24 h after DNA transfection, and cells were collected 48 h after DNA transfection. Firefly and *Renilla* luciferase activity was measured with an Infinite F200PRO plate reader (TECAN). Data are presented as firefly/*Renilla* luciferase activity.

Growth assays and cell cycle analysis. For growth assays, cells were seeded in 96-well plates (4,000 cells per well, 8 wells per sample) and fixed at the indicated time points with a crystal violet solution (0.05% w/v Crystal violet, 1% formaldehyde, 1% methanol in PBS) for 20 min at room temperature; stained cells were washed and air-dried. Crystal violet was extracted with 1% SDS (w/v in double-distilled H_2O, 100 µl per well) and absorbance at $\lambda = 595$ nm was measured.

To determine the fraction of cells in each phase of the cell cycle, subconfluent cells were trypsinized 48 h after siRNA transfection, fixed in cold 70% ethanol and stained with 0.02 mg ml^{-1} propidium iodide + 0.2 mg ml^{-1} RNase A in PBS. Stained cells were analysed on a FC500 cytofluorimeter (Beckman Coulter).

Soft-agar and mammosphere assays. For soft-agar assay, 10^4 MCF10A cells in complete growth medium with 0.35% agar were layered onto 0.5% agar beds in six-well plates; complete medium was added on top of cells and was replaced with fresh medium twice a week for 15 days. Colonies larger than 100 µm in diameter were counted as positive for growth. Thresholds were arbitrarily set to classify colonies according to their size.

For mammosphere formation assay, 1,000 cells cm^{-2} were seeded on ultralow-attachment plates (Costar), in DMEM/F12 supplemented with 10 ng ml^{-1} EGF,

DOI: 10.1038/ncb3216

5 μg ml^{-1} insulin, 0.5 μg ml^{-1} hydrocortisone, 52 μg ml^{-1} bovine pituitary extract and B27 supplement. Mammospheres were counted after one week.

Mice. Animal experiments were performed adhering to our institutional guidelines (CEASA, Comitato Etico per la Sperimentazione Animale, corresponding to our Animal Welfare Body).

For orthotopic transplantation experiments, MCF10A cells were injected into the abdominal mammary glands of 6–10-week-old *RAG*$^{-/-}$ female mice. For each injection, 10^6 cells were mixed 1:1 with Matrigel, in a final volume of 100 μl. Tumour growth in the injected site was monitored by repeated calliper measurements. Mice were euthanized after one month and tumours were explanted, fixed in 4% PFA and embedded in paraffin for histological analyses. The number of injections were: control (e.v.) $n=8$, +AP-1 $n=10$, +YAP $n=10$, +YAP+AP-1 $n=12$, +YAPS94A $n=6$, +YAPS94A+AP-1 $n=6$.

Yap1$^{fl/fl}$ mice were provided by D. Pan[58]. *K14–CreERT2* mice were provided by P. Chambon[38]. *Taz*$^{fl/fl}$ mice were described in ref. 33. Animals were genotyped with standard procedures[59], and with the recommended set of primers. To selectively ablate YAP/TAZ in epidermal keratinocytes of adult mice, mice carrying LoxP-site-containing *Yap* and *Taz* alleles were bred with hemizygous *K14–CreERT2*$^{tg/0}$ transgenic mice, to produce *K14–CreERT2*$^{tg/0}$; *Yap*$^{fl/fl}$; *Taz*$^{fl/+}$. 6–8-week-old mice (4 females and 5 males in each experimental group) received 3 intraperitoneal injections of tamoxifen (1 mg in 100 μl corn oil) to produce control (from *K14–CreERT2*$^{tg/0}$) or conditional Yap/Taz KO mice (from *K14–CreERT2*$^{tg/0}$; *Yap*$^{fl/fl}$; *Taz*$^{fl/+}$). Two weeks after tamoxifen injection, mice were shaved to synchronize the hair cycle and treated the day after with a single dose of DMBA (Sigma, 100 μg in 100 μl acetone). One week after DMBA application, TPA (Sigma, 5 μg in 100 μl acetone) was applied topically twice a week for up to 40 weeks. The number of tumours per mouse was recorded weekly. Tumours or skin explants were excised at the end of the DMBA/TPA treatment, fixed in 4% PFA and embedded in paraffin for histological sections. DNA was extracted from skin and genotyped with the recommended set of primers for *Yap* null allele (as in ref. 58), *Taz* null allele (as in ref. 33) and *K14–CreERT2* (for: 5′-TGGGAAAGTGTAGCCTGCAG-3′; rev: 5′-TCCCCTTGGCTTTCATCACC-3′; 182 bp).

All tested animals were included; no statistical method was used to predetermine sample size; no randomization or blinding was used.

Immunohistochemistry. Immunohistochemical staining was performed as described in ref. 60. Primary antibodies were anti-human Ki67 (Dako, M7240) and anti-human cytokeratin (Dako, M0821).

Reproducibility of experiments. ChIP-seq experiments contained two biological replicates, obtained from two independent experiments. For ChIP-qPCR, at least two independent experiments (each containing 2 biological replicates) were performed with similar results. For gene expression analysis with Affymetrix Microarrays four biological replicates were analysed for each sample. For qRT–PCR, 3 independent experiments (each with 2 biological replicates) were performed, with similar results. 3C experiments contained $n=3$ biological replicates and were repeated twice with similar results. Co-immunoprecipitation assays, DNA pulldown, western blots and PLA assays were performed three times with similar results. For luciferase assays, each experiment contained 2 biological replicates and was repeated at least three times independently with similar results. For growth assays, 8 independent replicate wells were analysed for each sample; each experiment was performed at least twice, with similar results. For cell cycle analysis, experiments contained $n=3$ biological replicates for each condition, and were repeated at least twice with similar results. Soft-agar assays contained $n=3$ biological replicates for each condition and were performed three times, with similar results. Mammosphere assays contained $n=6$ biological replicates for each condition and were performed three times, with similar results.

Luciferase data are presented as mean + s.d. of $n=4$ biological replicates from 2 experiments.

For all other experiments, results from one representative experiment are shown.

Accession numbers. ChIP-seq data is stored in the Gene Expression Omnibus under accession number GSE66081 for and gene expression data under GSE66082. All data from this study have been deposited in the GEO database under accession number GSE66083.

Accession numbers for public ChIP-seq and gene expression data sets used in this study are reported in Supplementary Tables 7 and 8, respectively.

37. Dupont, S. *et al.* Role of YAP/TAZ in mechanotransduction. *Nature* **474,** 179–183 (2011).
38. Li, M. *et al.* Skin abnormalities generated by temporally controlled RXRalpha mutations in mouse epidermis. *Nature* **407,** 633–636 (2000).
39. Dupont, S. *et al.* FAM/USP9x, a deubiquitinating enzyme essential for TGFbeta signaling, controls Smad4 monoubiquitination. *Cell* **136,** 123–135 (2009).
40. Martello, G. *et al.* A microRNA targeting dicer for metastasis control. *Cell* **141,** 1195–1207 (2010).
41. Azzolin, L. *et al.* Role of TAZ as mediator of Wnt signaling. *Cell* **151,** 1443–1456 (2012).
42. Schmidt, D. *et al.* ChIP-seq: using high-throughput sequencing to discover protein-DNA interactions. *Methods* **48,** 240–248 (2009).
43. Langmead, B., Trapnell, C., Pop, M. & Salzberg, S. L. Ultrafast and memory-efficient alignment of short DNA sequences to the human genome. *Genome Biol.* **10,** R25 (2009).
44. Li, Q., Brown, J. B., Huang, H. & Bickel, P. J. Measuring reproducibility of high-throughput experiments. *Ann. Appl. Stat.* **5,** 1752–1779 (2011).
45. Landt, S. G. *et al.* ChIP-seq guidelines and practices of the ENCODE and modENCODE consortia. *Genome Res.* **22,** 1813–1831 (2012).
46. Zhang, Y. *et al.* Model-based analysis of ChIP-Seq (MACS). *Genome Biol.* **9,** R137 (2008).
47. Harrow, J. *et al.* GENCODE: the reference human genome annotation for The ENCODE Project. *Genome Res.* **22,** 1760–1774 (2012).
48. Kharchenko, P. V., Tolstorukov, M. Y. & Park, P. J. Design and analysis of ChIP-seq experiments for DNA-binding proteins. *Nat. Biotechnol.* **26,** 1351–1359 (2008).
49. Heinz, S. *et al.* Simple combinations of lineage-determining transcription factors prime cis-regulatory elements required for macrophage and B cell identities. *Mol. Cell* **38,** 576–589 (2010).
50. Enzo, E. *et al.* Aerobic glycolysis tunes YAP/TAZ transcriptional activity. *EMBO J.* **34,** 1349–1370 (2015).
51. Irizarry, R. A. *et al.* Exploration, normalization, and summaries of high density oligonucleotide array probe level data. *Biostatistics* **4,** 249–264 (2003).
52. Dai, M. *et al.* Evolving gene/transcript definitions significantly alter the interpretation of GeneChip data. *Nucleic Acids Res.* **33,** e175 (2005).
53. Tusher, V. G., Tibshirani, R. & Chu, G. Significance analysis of microarrays applied to the ionizing radiation response. *Proc. Natl Acad. Sci. USA* **98,** 5116–5121 (2001).
54. Huang, F., He, J., Zhang, Y. & Guo, Y. Synthesis of biotin-AMP conjugate for 5' biotin labeling of RNA through one-step *in vitro* transcription. *Nat. Protoc.* **3,** 1848–1861 (2008).
55. Debnath, J., Muthuswamy, S. K. & Brugge, J. S. Morphogenesis and oncogenesis of MCF-10A mammary epithelial acini grown in three-dimensional basement membrane cultures. *Methods* **30,** 256–268 (2003).
56. Bodega, B. *et al.* Remodeling of the chromatin structure of the facioscapulohumeral muscular dystrophy (FSHD) locus and upregulation of FSHD-related gene 1 (FRG1) expression during human myogenic differentiation. *BMC Biol.* **7,** 41 (2009).
57. Zhang, H. *et al.* TEAD transcription factors mediate the function of TAZ in cell growth and epithelial-mesenchymal transition. *J. Biol. Chem.* **284,** 13355–13362 (2009).
58. Zhang, N. *et al.* The Merlin/NF2 tumor suppressor functions through the YAP oncoprotein to regulate tissue homeostasis in mammals. *Dev. Cell* **19,** 27–38 (2010).
59. Morsut, L. *et al.* Negative control of Smad activity by ectodermin/Tif1gamma patterns the mammalian embryo. *Development* **137,** 2571–2578 (2010).
60. Adorno, M. *et al.* A mutant-p53/Smad complex opposes p63 to empower TGFβ-induced metastasis. *Cell* **137,** 87–98 (2009).

nature cell biology

DOI: 10.1038/ncb3216

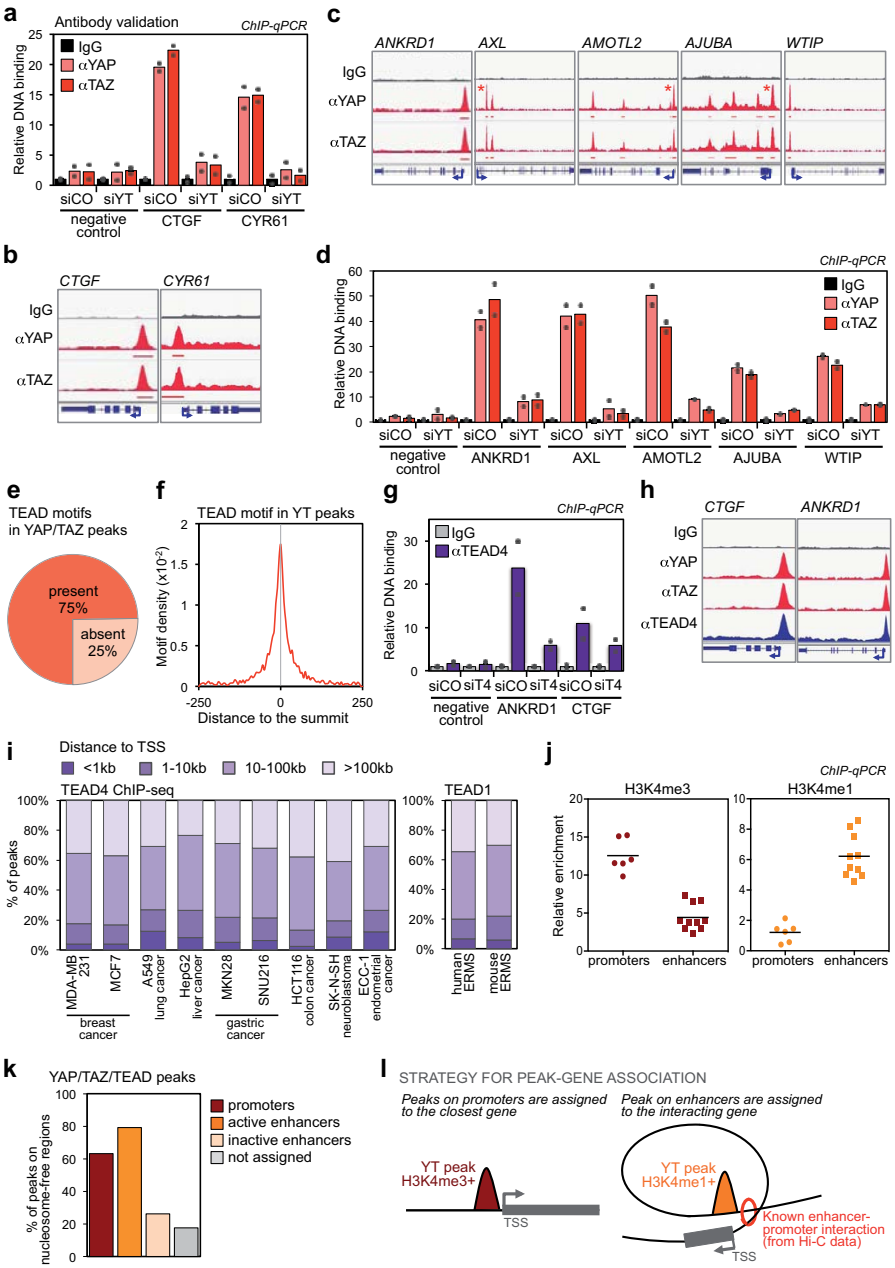

Supplementary Figure 1 Genome-wide identification of YAP/TAZ/TEAD binding sites. (a) ChIP-qPCR on the promoters of established YAP/TAZ direct targets showing the specificity of YAP and TAZ antibodies. *CTGF* and *CYR61* promoter sequences (but not a negative control locus) were enriched in YAP- and TAZ-immunoprecipitated chromatin, but not in negative control IP (IgG) or in chromatin obtained from YAP/TAZ-depleted cells. Relative DNA binding was calculated as fraction of input and normalized to IgG. Data from 2 biological replicates (individual data points and their mean) from one representative experiment are shown. (b-c) YAP/TAZ binding profiles and called peaks at positive control loci (*b*) and other known YAP/TAZ-regulated genes (c). Asterisks indicate peaks validated in (d). (d) Validation by ChIP-qPCR of YAP/TAZ binding sites identified through ChIP-seq. 2 biological replicates from one representative experiment are shown. (e) Percentage of YAP/TAZ peaks containing at least one known TEAD-binding motif. (f) Position of TEAD motif relative to the top of YAP/TAZ peaks. The curve shows the density of TEAD motifs at each position in a 500 bp window surrounding the summit of the corresponding YAP/TAZ peaks. (g) Specificity of TEAD4 antibody was assessed by ChIP-qPCR in control (siCO) and TEAD4-depleted MDA-MB-231 cells (siT4). 2 biological replicates from one representative experiment are shown. (h) ChIP-seq profiles, showing co-occupancy of *CTGF* and *ANKRD1* promoters by YAP/TAZ and TEAD4. (i) Genomic distribution of TEAD4 or TEAD1 ChIP-seq peaks relative to the closest TSS in the indicated cell types. ERMS=embryonal rhabdomyosarcoma. (j) ChIP-qPCR comparing the levels of H3K4me3 and H3K4me1 (normalized to total H3 levels) in a group of YAP/TAZ/TEAD-bound promoters and enhancers. Data points are the mean of two biological replicates from one representative experiment. "Promoters" are YAP/TAZ/TEAD peaks close to the TSS of *ANKRD1*, *AMOTL2*, *AXL*, *TK1*, *AJUBA* and *WTIP*; enhancers are YAP/TAZ/TEAD peaks 40841 (connected to *MYC* - see text and Supplementary Table 1), 40896 (*MYC*), 24736 (*GINS1*), 31079 (*CCNA2*), 16872, 16908, 16914 (*TOP2A*), 7673 (*CDCA5*), 7773 (*FOSL1*), 16878 (*CDC6*). (k) Percentage of YAP/TAZ/TEAD peaks localized in nucleosome-depleted regions, defined by FAIRE. (l) Schematic representation of the procedure used to identify candidate YAP/TAZ/TEAD direct target genes. See Methods for reproducibility of experiments.

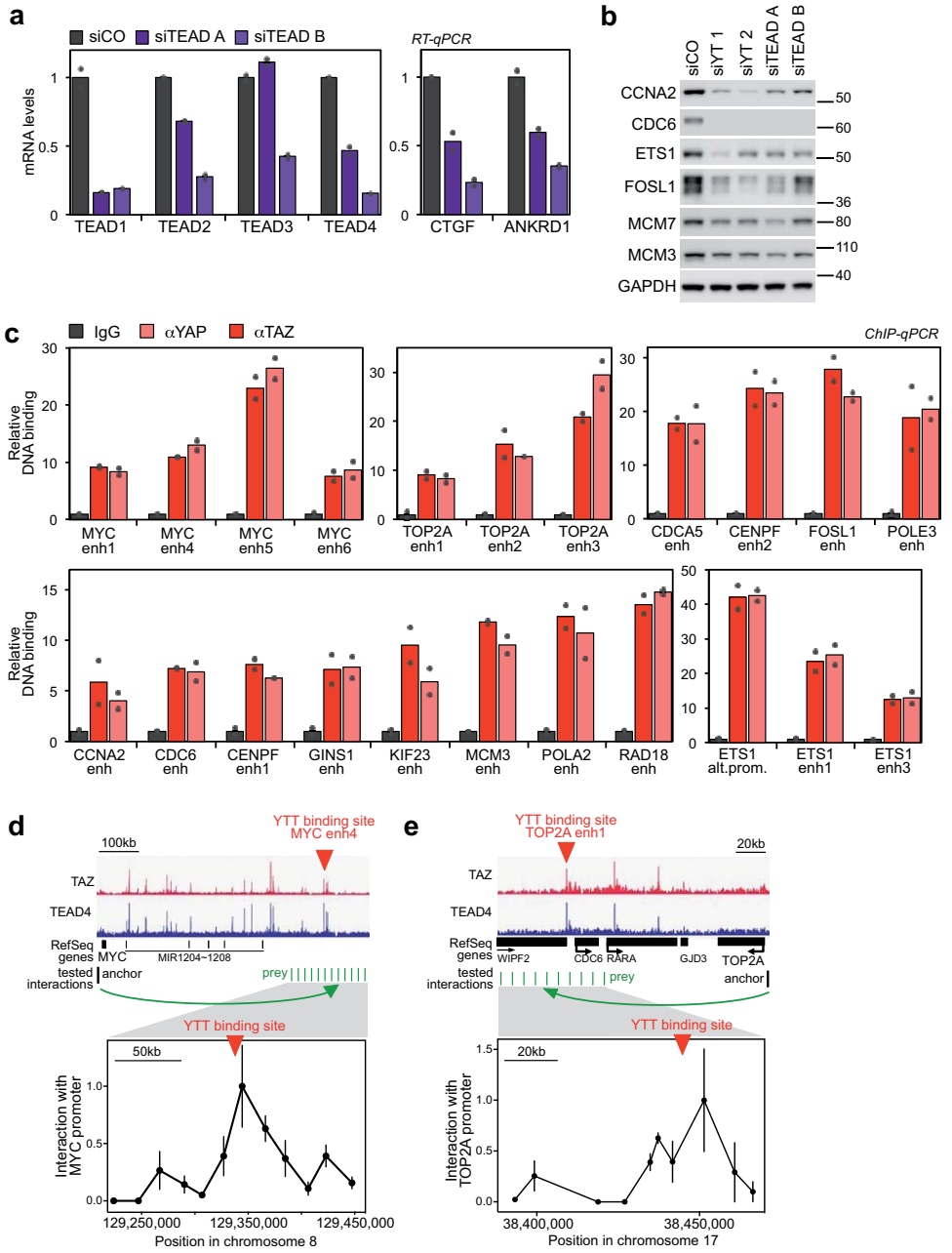

Supplementary Figure 2 YAP/TAZ/TEAD cell proliferation program. (a) mRNA levels (measured by qRT-PCR and normalized to *GAPDH*) for *TEAD1-4* in MDA-MB-231 cells transfected with siTEAD A or siTEAD B. Data from 2 biological replicates (individual data points and their mean) from one representative experiment are shown. The effectiveness of TEAD depletion was also evaluated by qRT-PCR for the expression of the YAP/TAZ/TEAD targets *CTGF* and *ANKRD1*. (b) Western blot for the indicated proteins in MDA-MB-231 cells transfected with control siRNA (siCO), YAP/TAZ siRNAs (siYT) or TEAD siRNAs (siTEAD). GAPDH serves as loading control. (c) ChIP-qPCR verifying YAP/TAZ binding to the enhancers associated with a subset of YAP/TAZ target genes presented in Figure 2b. Relative DNA binding was calculated as fraction of input and normalized to IgG; data from 2 biological replicates from one representative experiment are shown. See Supplementary Figure 1d for negative control locus. (d) Validation of the DNA looping interaction between the MYC promoter and a downstream YAP/TAZ/TEAD-occupied enhancer, using 3C assay. Data are presented as in Figure 2c. Data points are mean+SEM from n=3 biological replicates. (e) Validation of the DNA looping interaction between the TOP2A promoter and a downstream YAP/TAZ/TEAD-occupied enhancer, using 3C assay. Data are presented as in Figure 2c. Data points are mean+SEM from n=3 biological replicates. See Methods for reproducibility of experiments.

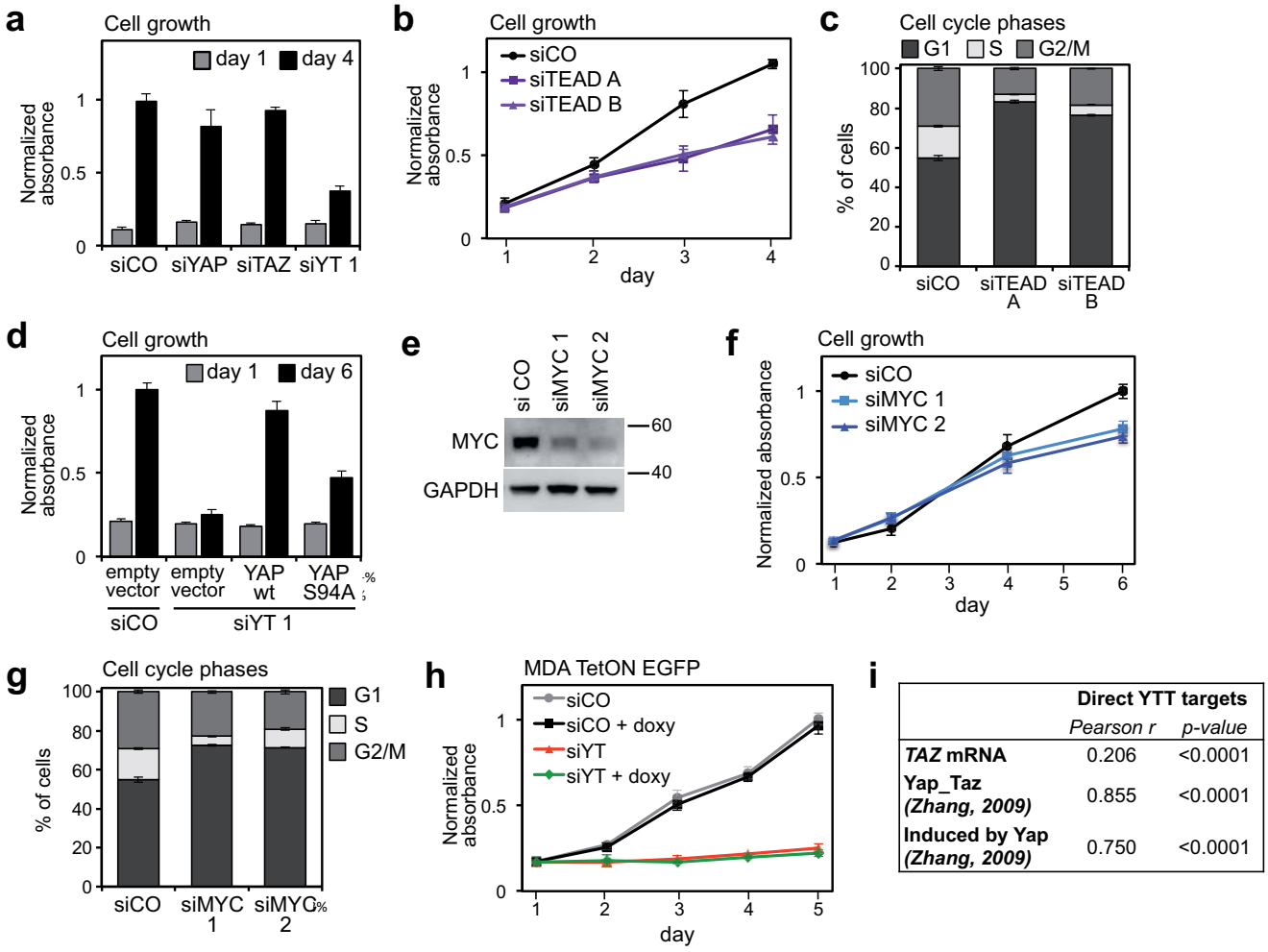

i

	Direct YTT targets	
	Pearson r	*p-value*
***TAZ* mRNA**	0.206	<0.0001
Yap_Taz *(Zhang, 2009)*	0.855	<0.0001
Induced by Yap *(Zhang, 2009)*	0.750	<0.0001

Supplementary Figure 3 Control of cell proliferation by YAP/TAZ, TEAD and their target MYC. (a) Growth of MDA-MB-231 cells transfected with control siRNA (siCO), YAP siRNA (siYAP), TAZ siRNA (siTAZ) or a combination of YAP and TAZ siRNAs (siYT). Data are mean+SD of n=8 biological replicates. (b) Growth curve of MDA-MB-231 cells transfected with control siRNA (siCO) or TEAD siRNAs (siTEAD). Data are mean+SD of n=8 biological replicates. (c) Percentage of MDA-MB-231 cells in G1, S and G2/M phases of cell cycle, as determined by flow-cytometric analysis. Cells were transfected with control (siCO) or TEAD siRNAs (siTEAD) 48hr before fixation. Data are mean+SD of n=3 biological replicates. (d) Sustained expression of YAP, but not of TEAD-binding deficient YAPS94A, rescues cell proliferation in YAP/TAZ-depleted cells. Empty-vector-, wild-type YAP- (wt) or YAPS94A-transduced MDA-MB-231 cells were transfected with control (siCO) or YAP/TAZ (siYT) siRNAs, as indicated. Proliferation was evaluated as in (a). Data are mean+SD of n=8 biological replicates. (e) Western blot showing Myc depletion in cells transfected with two MYC siRNAs. GAPDH serves as loading control. (f) Growth curve of MDA-MB-231 cells transfected with control siRNA (siCO) or MYC siRNAs (siMYC). Data are mean+SD of n=8 biological replicates. (g) Percentage of MDA-MB-231 cells in G1, S and G2/M phases of the cell cycle, as determined by flow-cytometric analysis. Cells were transfected with control (siCO) or MYC siRNAs (siMYC) 48h before fixation. Data are mean+SD of n=3 biological replicates. (h) MDA-MB-231 cells were transduced with lentiviral vectors encoding rtTA and doxycycline-inducible EGFP (MDA TetON EGFP) and transfected with control or YAP/TAZ siRNAs. Where indicated, EGFP expression was induced with 0.1 µg/ml doxycycline at the time of transfection. Cell growth was evaluated as in (a). Data are mean+SD of n=8 biological replicates. (i) Correlation between the expression of validated YAP/TAZ/TEAD (YTT) direct target gene signature and *TAZ* (*WWTR1*) mRNA or established YAP/TAZ signatures in breast cancer samples. Pearson correlation coefficients (r) and p-values are shown (one-tailed t test, p<0.0001 for all correlations). See Methods for reproducibility of experiments.

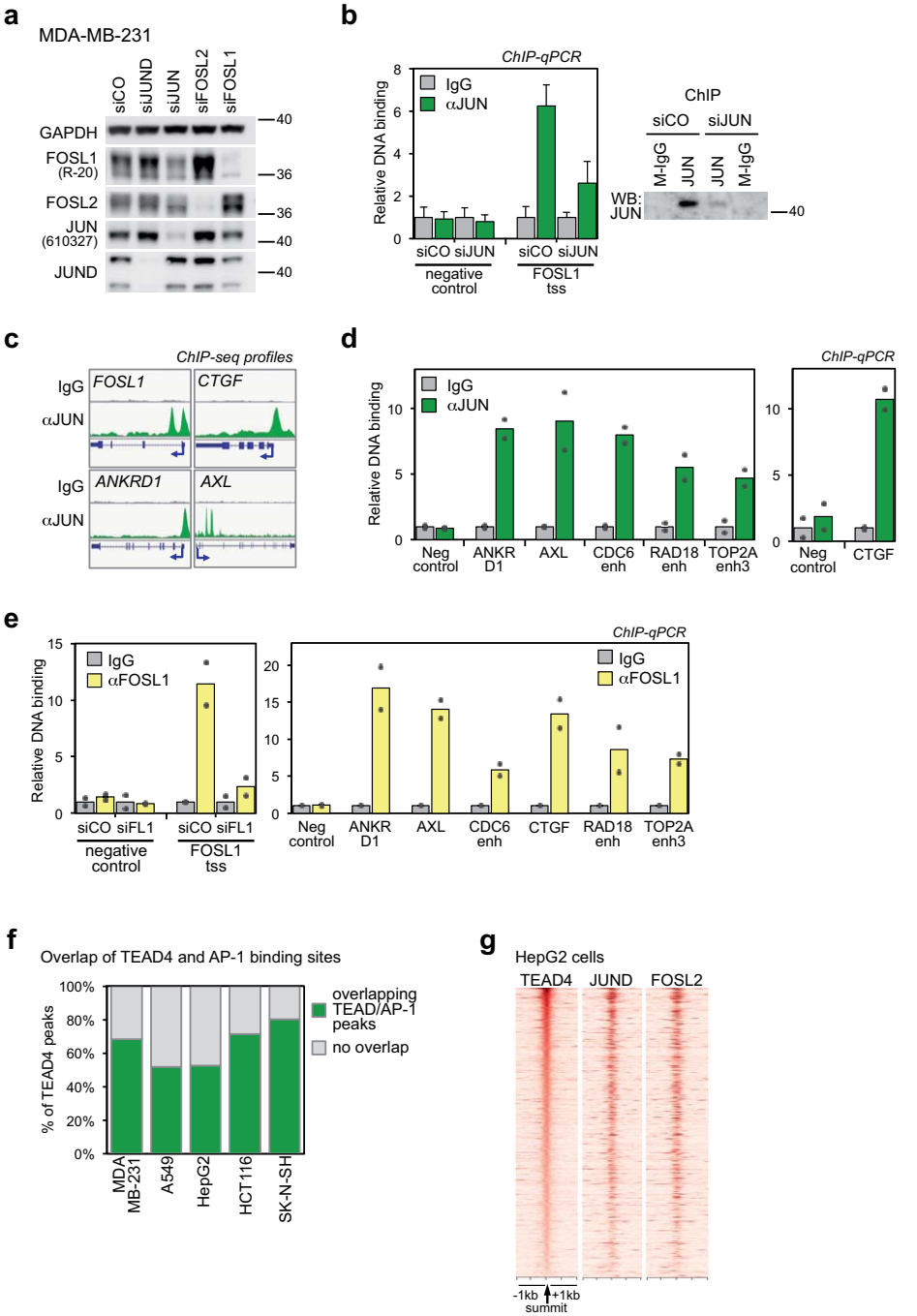

Supplementary Figure 4 Chromatin co-occupancy of YAP, TAZ, TEAD and AP-1 at the genome-wide level. (a) Western blot showing the specificity of antibodies recognizing AP-1 proteins used in this study. GAPDH serves as loading control. (b) Left: ChIP-qPCR on the promoter of the established AP-1 direct target *FOSL1* showing the specificity of JUN antibody. *FOSL1* promoter sequence was enriched in JUN-immunoprecipitated chromatin, but not in negative control IP (IgG) or in chromatin obtained from JUN-depleted cells. Relative DNA binding was calculated as fraction of input and normalized to IgG; data are presented as mean+SD of n=3 biological replicates. Right: Western blot showing that JUN is specifically immunoprecipitated by JUN antibody from crosslinked chromatin. (c) JUN binding profiles at *FOSL1* locus and known YAP/TAZ-regulated genes. (d) ChIP-qPCR validating JUN binding to the indicated genomic regions. Data from 2 biological replicates (individual data points and their mean) from one representative experiment are shown. (e) Left: ChIP-qPCR on the promoter of the established AP-1 direct target *FOSL1* showing the specificity of FOSL1 (R-20) antibody. Right: ChIP-qPCR showing FOSL1 binding to the same genomic regions occupied by JUN, as in (c). "siFL1" indicates cells transfected with FOSL1 siRNAs (serving as negative control). Data from 2 biological replicates from one representative experiment are shown. (f) Percentage of TEAD4 peaks overlapping with at least a ChIP-seq peak for a member of JUN and FOS families in MDA-MB-231 cells and in other cancer cell lines. (g) Heatmap representing TEAD4, JUND and FOSL2 ChIP-seq reads in HepG2 cells. TEAD4 binding sites are ranked from the strongest to weakest signal; a window of ±1kb centered on the summit of TEAD4 peaks is shown. See Methods for reproducibility of experiments.

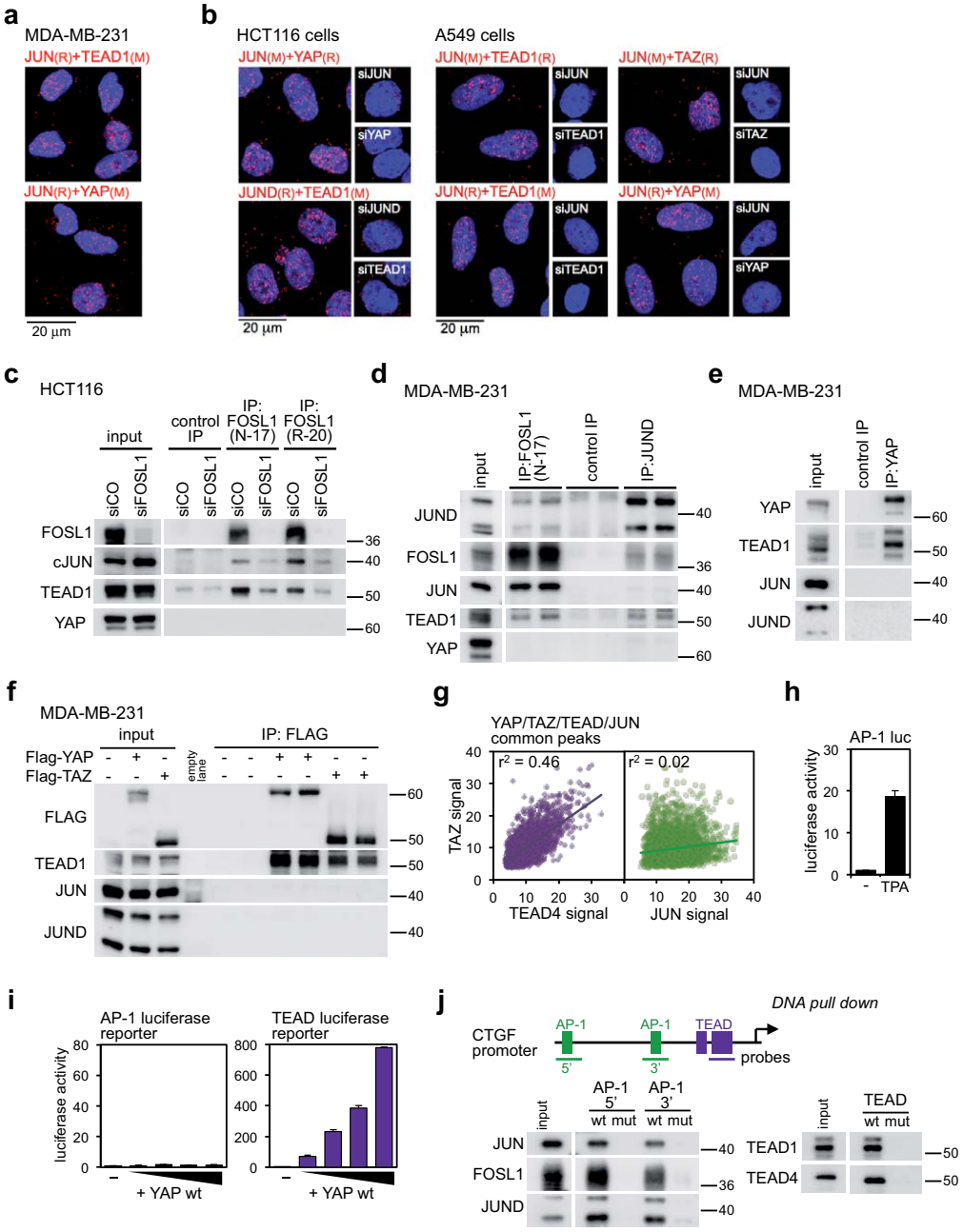

Supplementary Figure 5 Biochemical and functional interactions between YAP/TAZ/TEAD and AP-1 proteins. (a-b) *In situ* PLA detection of endogenous YAP/AP-1 and TEAD1/AP-1 interactions in MDA-MB-231 cells (a), HCT116 cells (b, left) and A549 cells (b, right). See Supplementary Table 6 for details about antibodies. Magnification is the same for all pictures. (c) TEAD1 co-precipitates with FOSL1 at endogenous protein levels in HCT116 cells. Two FOSL1 antibodies (N-17 and R-20) were used for IP. JUN is a positive control for co-IP. All samples were run on the same gel. (d) TEAD1, but not YAP, co-precipitates with FOSL1 and JUND immunocomplexes purified from MDA-MB-231 cells. Two independent immunoprecipitations were performed with FOSL1 (N-17) and JUND antibodies, or with control IgGs. Lanes 4 and 5 are also presented in Figure 3h; all samples were run on the same gel. (e) JUN and JUND cannot be detected in YAP immunocomplexes purified from MDA-MB-231 cells. TEAD1 is a positive control for co-IP. All samples were run on the same gel. (f) JUN and JUND cannot be detected in FLAG-YAP or FLAG-TAZ immunocomplexes purified from MDA-MB-231 cells. TEAD1 is a positive control for co-IP. (g) Linear correlation between the signal of YAP/TAZ peaks and TEAD4 or JUN peaks in the common binding sites. r^2 is the coefficient of determination of the correlation (h) AP-1 luciferase reporter (AP-1 luc) is activated by treatment with TPA in HEK293 cells. Data are mean+SD of n=4 biological replicates from 2 independent experiments. (i) HEK293 cells were transfected with increasing doses of YAP-expressing vector, and with an AP-1 (pAP1-luc, left) or TEAD (8xGTIIC-lux, right) luciferase reporter. Data are normalized to control sample ("-") and are presented as mean+SD of n=4 biological replicates from 2 independent experiments. (j) AP-1 or TEAD fail to bind to *CTGF* promoter after mutation of their cognate binding sites. Panels are Western blot analyses of the indicated endogenous proteins from MDA-MB-231 nuclear extracts, purified by DNA-pull down using biotinylated DNA probes designed on the sequence of *CTGF* promoter. See Supplementary Figure 7 for uncropped Western blots, and Methods for reproducibility of experiments.

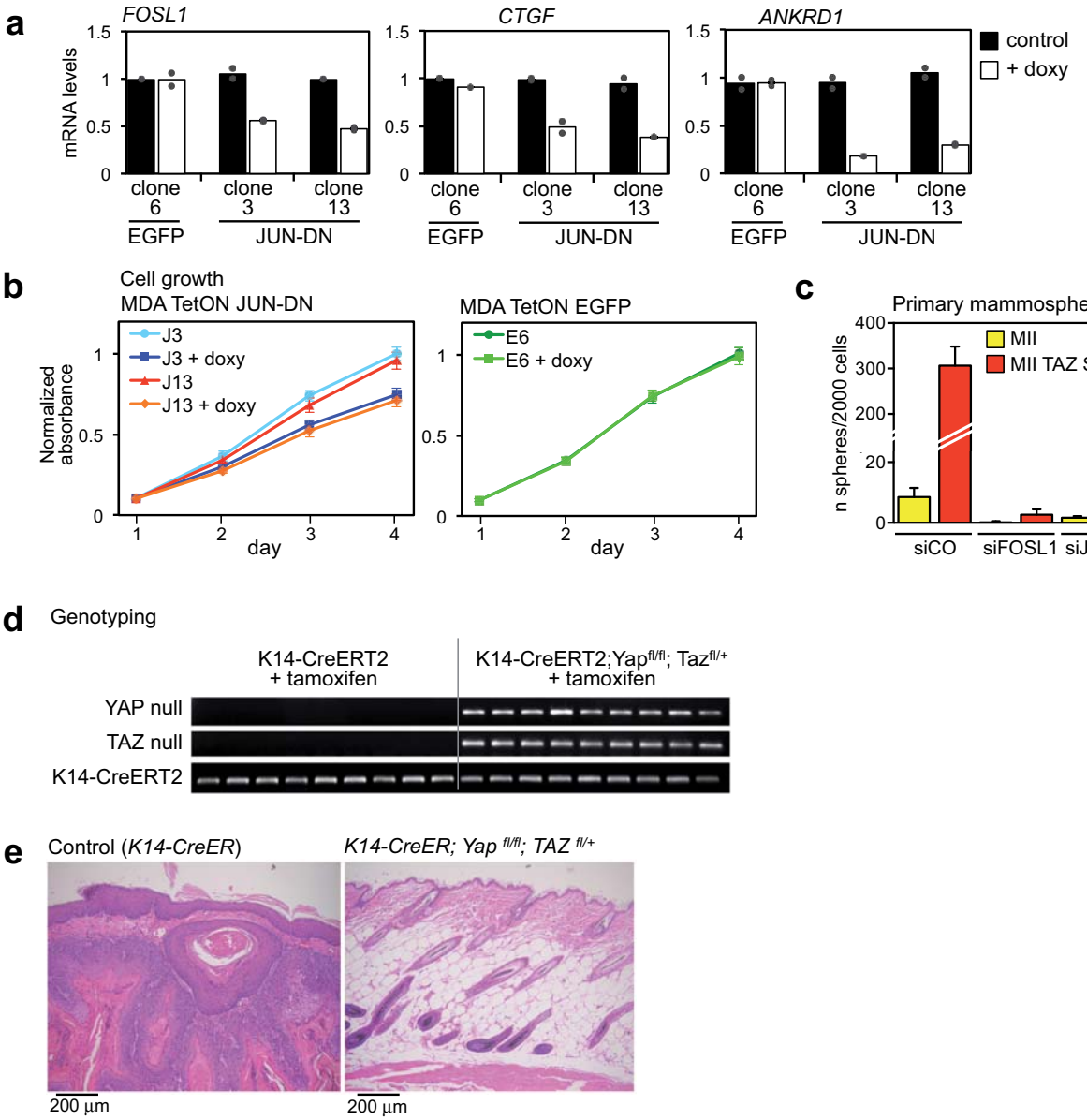

Supplementary Figure 6 Role of YAP/TAZ and AP-1 in oncogenic growth. (a) MDA-MB-231 cells were transduced with rtTA and doxycycline inducible JUN-DN (MDA TetON JUN-DN); clones were established to ensure high and uniform expression of JUN-DN upon doxycycline treatment. Similarly, clones of EGFP-expressing cells were generated as control (MDA TetON EGFP). Levels of the indicated transcripts were evaluated by qRT-PCR in cells untreated or exposed to doxycycline for 48h. mRNA levels are normalized to *GAPDH*. Data from 2 biological replicates (individual data points and their mean) from one representative experiment are shown. Downregulation of *FOSL1* transcript is a positive control for inhibition of AP-1 activity. *ANKRD1* and *CTGF* expression diminishes in doxycycline-treated MDA TetON JUN-DN cells, coherently with results of luciferase reporters in Figure 4i. (b) Growth rate of MDA TetON JUN-DN cells decreases upon JUN-DN induction with doxycycline (left panel); as control, EGFP induction has no effect (right panel). Data are mean+SD of n=8 biological replicates. (c) Control and TAZS89A-overexpressing MII cells were transfected with the indicated siRNAs and tested for mammosphere formation. Data are presented as mean+SD of n=6 biological replicates from a representative experiment. (d) Genomic DNA was extracted from the skin of control mice (n=9, left) and conditional knockout mice (n=9, right) to verify tamoxifen-induced recombination of *Yap* and *Taz* loci. Panels are PCR bands for the indicated alleles. (e) Magnifications of representative H&E-stained sections of skin tumors shown in Figure 6b. Left: detail of a SCC area in a tumor of treated control mice. Right: DMBA/TPA-treated skin from YAP/TAZ conditional knockout mice has a normal histological appearance. See Methods for reproducibility of experiments.

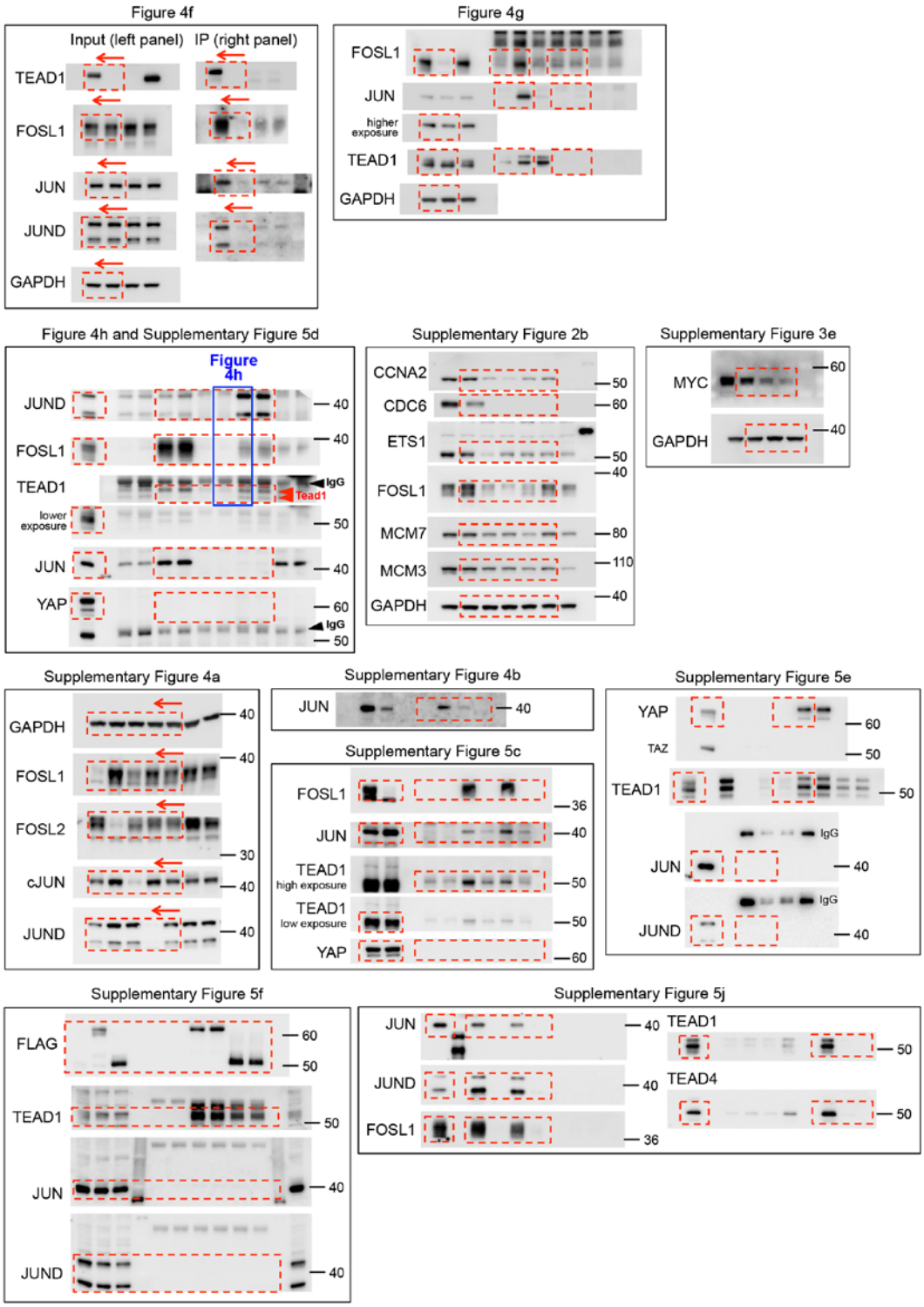

Supplementary Figure 7 Uncropped Western blots. Uncropped images of immunoblots displayed in the main and supplementary figures. Dashed boxes indicate areas that were cropped.

Supplementary Table Legends

Supplementary Table 1. TF motifs in YAP/TAZ peaks, and in shared YAP/TAZ and TEAD4 binding sites.
Results of *de novo* motif finding in common YAP/TAZ binding regions, and in YAP/TAZ binding regions also shared with TEAD4. Colums are: A) motif logo; B) p-value; C) percentage of peaks containing the motif; D) TFs predicted to bind the sequence indicated in A.

Supplementary Table 2. YAP/TAZ/TEAD peaks.
Full list of YAP/TAZ/TEAD common binding sites. Columns are: A) peak ID in αYAP ChIP-seq; B) peak ID in αTAZ ChIP-seq; C) peak ID in αTEAD4 ChIP-seq; D-F) genomic coordinates of the peak in αTAZ ChIP-seq; G) distance to the closest TSS of the peak in αTAZ ChIP-seq; H) classification of the peak as "promoter", "enhancer", "not assigned" according to H3K4me1 and H3K4me3 levels; I) classification of the peak as "active", "inactive", "not assigned" according to H3K27ac levels; J) overlap with FAIRE-seq peaks (0=no; 1=yes); K) target gene assigned by the method depicted in Supplementary Figure 1l; H) corresponding peak in αJUN ChIP-seq.

Supplementary Table 3. list of YAP/TAZ/TEAD direct target genes.
Full list of genes associated to at least one YAP/TAZ/TEAD binding site, and down-regulated in YAP/TAZ-depleted MDA-MB-231 cells.

Supplementary Table 4. Gene Ontology analysis of YAP/TAZ/TEAD direct target genes.
Full list of GO terms associated with YAP/TAZ/TEAD direct target genes. "Cell proliferation" and "RNA metabolism and transport" indicate the two categories in which GO terms were grouped.

Supplementary Table 5. YAP/TAZ/TEAD direct positive target genes included in the category "cell proliferation".
Full list of YAP/TAZ/TEAD direct positive targets involved in the control of cell growth. For each gene, the presence of an E2F motif in the promoter is also indicated.

Supplementary Table 6. Antibodies.
List of antibodies used in this study.

Supplementary Table 7. Public ChIP-seq datasets re-analyzed in this study.
Accession numbers of published ChIP-seq datasets re-analyzed in this study. References are listed in "Supplementary References".

Supplementary Table 8. Breast cancer datasets.
Accession numbers for breast cancer datasets (original datasets and revised cohorts). References are listed in "Supplementary References".

Supplementary Table 9. Oligonucleotide sequences.
Sequences of siRNAs, PCR primers, probes for DNA pull down, and the list of TaqMan assays used in this study.